Complex processes of cryptic speciation in mouse lemurs from a micro-endemism hotspot in Madagascar

Running title: Cryptic speciation in mouse lemurs

Dominik Schüßler[1#], Jordi Salmona[2#], Marina B. Blanco[3,4#], Jelmer Poelstra[4#], George P. Tiley[4#], Jean B. Andriambeloson[5], Olivier Bouchez[6], C. Ryan Campbell[4†], Paul D. Etter[7], Amaia Iribar[2], Paul A. Hohenlohe[8], Kelsie E. Hunnicutt[4@], Eric A. Johnson[7], Peter A. Larsen[4&], Jasmin Mantilla-Contreras[1], Sophie Manzi[2], Alexandra Miller[9], Blanchard Randrianambinina[10,11], David W. Rasolofoson[10], Amanda R. Stahlke[8], David Weisrock[12], Rachel C. Williams[3,4], Lounès Chikhi[2,9], Edward E Louis Jr.[13], Anne D. Yoder[4]*, Ute Radespiel[14]*

[1]: Research Group Ecology and Environmental Education, Institute of Biology and Chemistry, University of Hildesheim, Universitaetsplatz 1, 31141 Hildesheim, Germany

[2]: CNRS, Université Paul Sabatier, IRD; UMR5174 EDB (Laboratoire Évolution & Diversité Biologique), 118 route de Narbonne, 31062 Toulouse, France

[3]: Duke Lemur Center, Duke University, Durham, NC 27705, USA

[4]: Department of Biology, Duke University, Durham, NC 27708, USA

[5]: Zoology and Animal Biodiversity, University of Antananarivo, Antananarivo 101, Madagascar

[6]: INRA, US 1426, GeT-PlaGe, Genotoul, Castanet-Tolosan, France

[7]: Institute of Molecular Biology, University of Oregon, Eugene, OR, USA

[8]: Institute for Bioinformatics and Evolutionary Studies, Department of Biological Sciences, University of Idaho, Moscow, ID 83844, USA

[9]: Instituto Gulbenkian de Ciência, Rua da Quinta Grande, 6, 2780-156 Oeiras, Portugal

[10]: Groupe d'Etude et de Recherche sur les Primates de Madagascar (GERP); BP 779, Antananarivo 101, Madagascar

[11]: Faculté des Sciences, University of Mahajanga, Mahajanga, Madagascar

[12]: Department of Biology, University of Kentucky, Lexington, KY, 40506, USA

[13]: Grewcock Center for Conservation and Research, Omaha's Henry Doorly Zoo and Aquarium, Omaha, NE

[14]: Institute of Zoology, University of Veterinary Medicine Hannover, Buenteweg 17, 30559 Hannover, Germany

#: joint first authors

*: joint senior authors (corresponding authors)

@: current address: Department of Biological Sciences, University of Denver, Denver, CO 80208

&: current address: Department of Veterinary and Biomedical Sciences, University of Minnesota, Saint Paul, MN 55108

†: current address: Department of Evolutionary Anthropology, Duke University, Durham, NC 27708, USA

Corresponding authors:

Ute Radespiel, Institute of Zoology, University of Veterinary Medicine Hannover, Germany, email: ute.radespiel@tiho-hannover.de

Anne D. Yoder, Department of Biology, Duke University, Durham, NC, USA, email: anne.yoder@duke.edu

Author contributions:

- *Conception and design of study:*

DS, JS, LC, JP, GPT, JMC, ADY, UR

- *Data collection:*

DS, MBB, JBA, AM, EELJ, DWR, BR collected samples in the field.

- *Data analysis and interpretation:*

DS, JS, LC, OB, PE, CRC, PAL, ARS, DW, AIP, PH, KEH, EJ, SM, RCW, EELJ, UR generated sequencing data.

DS, JS, MBB, JP, GPT, ADY, UR conducted and interpreted morphometric, population genetic and phylogenetic analyses.

- *Drafting and revising manuscript:*

DS, JS, JP, GPT, ADY, UR drafted the manuscript.

All co-authors revised and agreed on the last version of the manuscript.

Data Accessibility Statement:

XXX

Abstract

Species delimitation is ever more critical for assessing biodiversity in threatened regions of the world, with cryptic species offering one of the greatest challenges. Our study focuses on a conservation hotspot in northeastern Madagascar where at least five species of mouse lemur (*Microcebus* spp.) occur, some of them in sympatry. One of these, *M. jonahi*, is described here as new to science and is accompanied by a complete genome. While morphometric analyses confirmed the cryptic nature of taxa, phylogenetic and population genetic analyses clarified species boundaries despite some interspecific gene flow, including introgression of mtDNA. The sister species pair that includes *M. jonahi* passed all tests of species delimitation, whereas the other pair showed more marginal results. This is at least partially due to differences in effective population sizes, which affect coalescence rates and thus influence the recently introduced genealogical divergence index (*gdi*). Whole-genome and RADseq analyses suggest a precipitous decline in effective population sizes associated with successive divergence events of lineages leading to the micro-endemics *M. jonahi* and its sister species, giving rise to grave conservation concern for both. Finally, our study demonstrates the power of genomic species delimitation approaches for revealing hidden evolutionary processes in cryptic species complexes.

Keywords: effective population size, *Microcebus jonahi*, cryptic species, multispecies coalescent, species delimitation, speciation

Introduction

The investigation of evolutionary mechanisms that drive speciation heavily depends on accurately delimiting species. In the past decade, both the theory and the methods for species delimitation have seen substantial progress and stimulating debate (Yang and Rannala 2010; Edwards and Knowles 2014; Barley et al. 2017; Sukumaran and Knowles 2017; Jackson et al. 2017; Luo et al. 2018; Leaché et al. 2019). In parallel, genomic technologies have yielded a powerful toolkit for examining complex evolutionary processes with sophisticated statistical approaches, such as detecting the presence and magnitude of gene flow before or after speciation events (Payseur and Rieseberg 2016; Dalquen et al. 2017; Wen et al. 2018).

Mouse lemurs (*Microcebus* spp.) provide an intriguing system for investigating the evolutionary processes that give rise to new species, given that they show patterns of rapid diversification, cryptic morphology, and overlapping geographic distributions (e.g., Zimmermann et al. 1998; Rasoloarison et al. 2000; Radespiel et al. 2008). More generally, Madagascar is a global biodiversity hotspot (Myers et al. 2000; Goodman and Benstead 2005; Estrada et al. 2017) that is severely threatened (e.g., Schwitzer et al., 2014, Waeber et al. 2016) and thus species delimitation in mouse lemurs is of direct conservation interest. Mouse lemurs are small-bodied (approximately 40 - 80 g), nocturnal primates whose high species diversity was long overlooked due to their cryptic nature (Zimmermann and Radespiel 2014). With the introduction of genetic analyses, it became feasible to identify diverging lineages despite minimal morphological differences. This has led to the description of many new species of mouse lemur, with a total of 24 species now recognized (Zimmermann et al. 1998; Rasoloarison et al. 2000; Yoder et al. 2000; Olivieri et al.

2007, Louis et al. 2006, 2008; Radespiel et al. 2008, 2012, Rasoloarison et al. 2013, Hotaling et al. 2016, Louis and Lei 2016).

Many taxonomic descriptions have relied strongly, if not entirely, on mitochondrial sequence divergence to delimit species. This approach is widely regarded as problematic, however, given that the mitogenome represents only a single, non-neutral, non-recombining locus whose gene tree may not represent the underlying species tree (e.g., Pamilo and Nei 1988; Maddison 1997). Mitochondria are also maternally inherited and therefore susceptible to effects of sex-biased dispersal (e.g., Dávalos and Russell 2014), which is prevalent in mouse lemurs (Radespiel et al. 2001). To further complicate matters, previous attempts to resolve relationships using sequences from nuclear markers were not successful due to high gene tree discordance consistent with strong incomplete lineage sorting (e.g., Heckman et al. 2007; Weisrock et al. 2010). But now, with modern sequencing techniques, investigators can sample thousands of loci across multiple individuals, which provides power for simultaneously resolving phylogenetic relationships and for estimating demographic parameters such as divergence times, effective population sizes, and rates of gene flow — even among closely related species (e.g., Pedersen et al. 2018; Palkopoulou et al. 2018).

The power of genomic data for delimiting species has been further enhanced by methods that leverage the multispecies coalescent (MSC) model (Pamilo and Nei 1988; Rannala and Yang 2003). Even so, recent work has pointed out that MSC methods, such as BPP (Yang and Rannala, 2010; Flouri et al., 2018) do not consider an alternative hypothesis of strong population structure when assigning species boundaries (Sukumaran and Knowles 2017; Jackson et al. 2017; Leaché et al. 2019; Chambers and Hillis 2019). To overcome this issue, Jackson et al. (2017) proposed a

heuristic criterion, the genealogical divergence index (*gdi*), with Leaché et al. (2019) further suggesting that *gdi* helps to differentiate between species-level divergence and population structure. These analytical developments are crucial to our ability to recognize mechanisms that drive the speciation process, despite the challenge of separating evolutionary lineages without universally agreed criteria (de Queiroz 2007).

Though mouse lemurs have been extensively studied in western Madagascar (e.g., Zimmermann et al. 1998; Rasoloarison et al. 2000; Olivieri et al. 2007), the diversity and geographic distributions of species along the eastern coast have only recently received as much attention. Studies from the past decade show that this region contains rich species diversity for mouse lemurs, with several new species described (Kappeler et al. 2005; Louis et al. 2006; Radespiel et al. 2008, 2012; Rasoloarison et al. 2013; Hotaling et al. 2016). In particular, Radespiel et al. (2008) surveyed the forests of the Makira region (`Fig. 1`) and found evidence for three different lineages occurring in sympatry, a phenomenon previously undocumented for mouse lemurs. One of these was identified as *M. mittermeieri*, while the second was newly described as *M. macarthurii*. A third lineage (*M.* sp. #3) was hypothesized to be a new species based on mitochondrial DNA (mtDNA) sequence data but could not be formally described given that only a single individual was sampled.

In this study, we revisit the Radespiel et al. (2008) findings by expanding the geographic and species-level sampling to reconstruct the evolutionary history of the mouse lemur lineages inhabiting this region and to test the hypothesis that *M.* sp. #3 represents a new species. We also provide a novel whole genome for this hypothesized new species thus allowing for a detailed conservation genomic analysis. Our study therefore represents the most intensive examination to

159 date of speciation dynamics within this cryptic species radiation, with the additional benefit of
160 yielding an intimate view of conservation dynamics in a biodiversity hotspot in northeastern
161 Madagascar.

Materials and methods

Study sites and sampling

Microcebus individuals were sampled between 2008 and 2017 at seven rain forest sites (50-979 m a.s.l.; Kottek et al. 2006) in the Analanjirofo and Sava regions of northeastern Madagascar (Fig. 1; Tab. S1). All study sites harbor a variety of habitats ranging from undisturbed near-primary rain forest to heavily degraded secondary shrub-, grass- and fern-lands (Radespiel et al. 2008; Miller et al. 2018; Schüßler et al. 2018). Additional samples were used from Riamalandy, Zahamena National Park (NP), Betampona Strict Nature Reserve (SNR) and Tampolo (Louis et al. 2006; Weisrock et al. 2010; Louis and Lei 2016; Fig. 1). With this sampling strategy, we expect to detect all mouse lemur species that occur in the region. These are (from north to south) *M. mittermeieri*, *M. macarthurii*, *M.* sp. #3, *M. lehilahytsara* and *M. simmonsi* (Fig. 1). *Microcebus murinus,* which occurs throughout western and southern Madagascar, was used as an outgroup for the analyses.

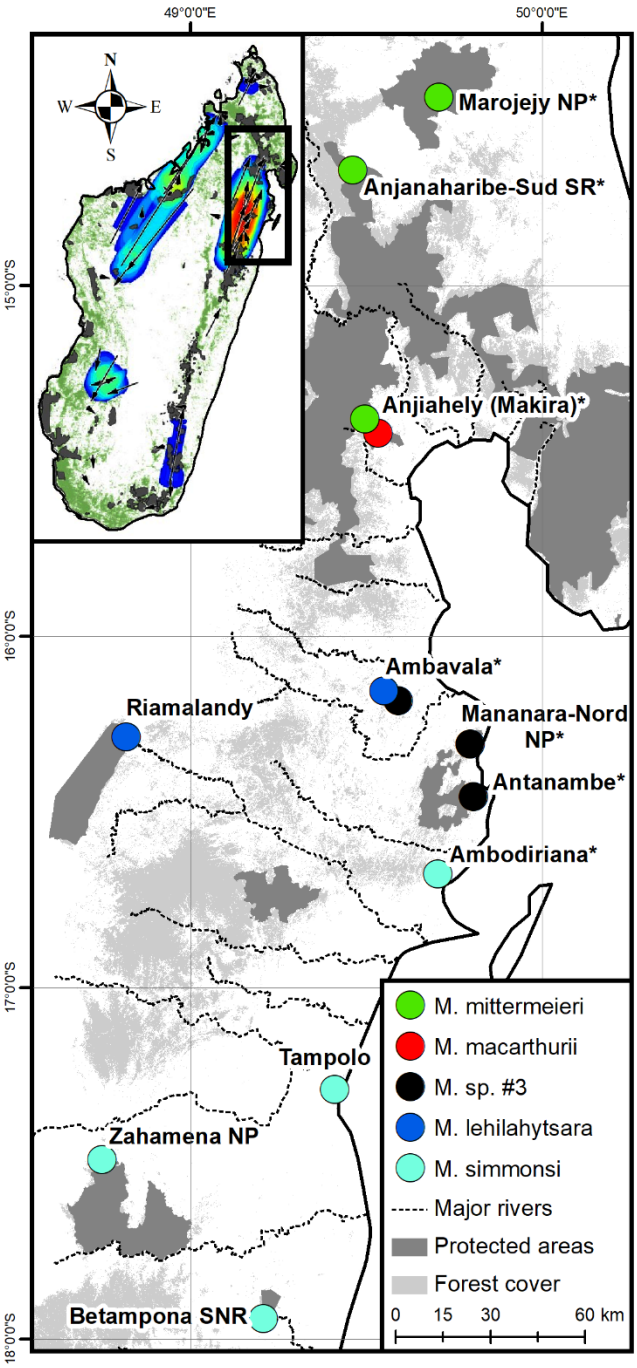

Figure 1: Sampling sites in northeastern Madagascar. New sampling locations are marked with *. The region coincides with a conservation hotspot for lemurs (see heat map in the inlay with warm colors representing conservation concern based on predicted range shifts in a large number of lemur species reproduced from Brown and Yoder 2015). Forest cover in 2018 derived from Schüßler et al. (under review).

182 **Sequencing, assembly, and annotation of a *M.* sp. #3 draft genome**

183 The genome of one individual of *M.* sp. #3 sampled from Mananara-Nord NP (Tab. S2) was
184 sequenced with a single 500bp insert library on a single lane of an Illumina HiSeq 3000 with
185 paired-end 150bp reads. We used MaSuRCA v3.2.2 (Zimin et al. 2013) for contig assembly and
186 SSPACE (Boetzer et al. 2011) for scaffolding, which uses BOWTIE (Langmead et al. 2009) to
187 realign short reads to the *de novo* assembly in order to potentially correct erroneously joined
188 contigs. Quality control and annotation of the draft genome is described in the Supplementary
189 Material. Scaffolds potentially containing mitochondrial or X-chromosome sequence data were
190 removed for downstream analyses (see Supplementary Methods).

191

192 **RADseq laboratory procedures and data processing**

193 We generated Restriction site Associated DNA sequencing (RADseq) libraries using the *Sbf*I
194 restriction enzyme, following three protocols (Supplementary Methods, Tab. S1). Cleaned
195 sequences were aligned to *M.* sp. #3 genome and to the *M. murinus* mitogenome (Lecompte et al.
196 2015; see Supplementary Methods for further details).

197

198 We used two fundamentally distinct approaches for genotyping to ensure robustness of our
199 results to variant calling errors. First, we estimated genotype likelihoods (GL) with ANGSD
200 v0.92 (Nielsen et al. 2012; Korneliussen et al. 2014). ANGSD retains information about
201 uncertainty in base calls, which alleviates some issues commonly associated with RADseq data
202 such as unevenness in sequencing depth and allele dropout (Lozier 2014; Pedersen et al. 2018;
203 Warmuth and Ellegren 2019). Second, we called genotypes with GATK v4.0.7.0 (dePristo et al.
204 2011), and filtered GATK genotypes following the "FS6" filter of O'Leary et al. (2018; see
205 Supplementary Methods for further details).

206

207 Three mtDNA fragments [Cytochrome Oxidase II (COII), Cytochrome B (cytB), d-loop] were
208 amplified and Sanger sequenced for additional phylogenetic analyses. For further details on
209 sequencing and genotyping procedures, see the Supplementary Material.

210

211 **Mutation rate and generation time**

212 To convert coalescent units from BPP and G-PhoCS analyses into absolute times and population
213 sizes, we used empirical estimates of mutation rate and generation time, but used uncertainty in
214 estimates to construct distributions rather than using a single point estimate for BPP and G-
215 PhoCS results. For each sampled generation of the MCMC chain, we drew a random number
216 from the mutation rate and generation time distributions, to better reflect our uncertainty in
217 absolute estimates. A recent pedigree-based estimate of mutation rate in *M. murinus* (Campbell et
218 al. 2019) found a mean of 1.64×10^{-8} with a 95% CI of 1.41×10^{-8} to 1.98×10^{-8}. We roughly
219 capture this mutation rate variation with a normal distribution that has a mean of 1.64 and a
220 standard deviation of 0.08. For generation time, two estimates were available for *Microcebus*. *M.*
221 *rufus* was estimated to have an average generation time of 4.5 years calculated from survival data
222 (Zohdy et al. 2014; Yoder et al. 2016), and 2.5 years was estimated for *M. murinus* using average
223 parent age based on capture-mark-recapture and parentage data in the wild (Radespiel et al. in
224 revision). We used a lognormal distribution with a mean of ln(3.5) and standard deviation of
225 ln(1.16). MSMC parameter estimates were converted using the point estimates.

226

227 **Phylogenetic analyses**

228 We used three phylogenetic approaches to infer relationships among lineages and to provide a
229 framework for subsequent species delimitation analyses. Phylogenetic analyses were conducted

via (1) maximum likelihood (RaxML v8.2.11; Stamatakis 2014), (2) a MSC method that is statistically consistent and uses phylogenetic invariants (SVDquartets in PAUP v4a163, Chifman and Kubatko 2014), and (3) a full-likelihood MSC method for biallelic data that does not require joint gene tree estimation (SNAPP v1.3.0; Bryant et al. 2012). Analyses with RAxML and SVDquartets used all available individuals, whereas SNAPP analyses were only performed with subsets of individuals for computational feasibility. Specifically, a 12-individual dataset that used two samples per species, and a 22-individual dataset with four samples per species were analyzed with SNAPP (Tab. S1). All analyses used *M. murinus* samples as outgroup. Phylogenetic software details are given in the Supplementary Material.

Species delimitation

Model-based inference with the MSC

We used SNAPP to test if the two pairs of sister taxa, *M.* sp. #3 – *M. macarthurii* and *M. mittermeieri* – *M. lehilahytsara*, could be delimited at the molecular level using Bayes factors (Leaché et al. 2014). Marginal likelihood estimation used stepping stone sampling (Xie et al. 2011) with 20 steps for both the 12- and 22- individual datasets, and we interpreted 2ln Bayes factors greater than six as strong evidence for a given model (Kass and Raftery 1995). We tested two hypotheses: the first considered the two taxa in each species pair as separate species, and the second considered them as belonging to the same species.

We also applied guided species delimitation analyses with BPP (Yang and Rannala 2010; Rannala and Yang 2013) based on the species tree estimated by SVDquartets and SNAPP but using analytical integration of population sizes (Hey and Nielsen 2007). MCMC options and prior choices for analyses are detailed in the Supplementary Material. Because BPP uses

254 substitution models not suitable for SNP data, we created full-sequence fasta files based on the
255 GATK genotypes using a series of in-house scripts
256 (https://github.com/jelmerp/msp3/tree/master/vcf2fullfasta; Supplementary Material).
257
258 BPP parameter estimates from the 12-individual dataset with the MSC were used to compute the
259 genealogical divergence index (*gdi*, Jackson et al. 2017; Leaché et al. 2019) for *M.* sp. #3 – *M.*
260 *macarthurii* and *M. lehilahytsara* – *M. mittermeieri*. We calculated *gdi* as in Leaché et al. (2019),
261 using their equation 7 ($gdi = 1-e^{-2\tau/\theta}$), where $2\tau/\theta$ represents the population divergence time
262 between taxa A and B in coalescent units, and θ is taken for a focal taxon (A or B). Again, as in
263 Leaché et al. (2019), *gdi* was calculated twice for each species pair, using each species as the
264 focal taxon once. We computed *gdi* using τ and θ parameter estimates for each posterior sample
265 from independent BPP chains, to directly incorporate uncertainty in the τ and θ estimates.
266 Jackson et al. (2017) suggested the following guidelines for the interpretation of *gdi* values: the
267 focal taxon pair is unambiguously a single species for $gdi < 0.2$, is unambiguously two separate
268 species for $gdi > 0.7$, and falls in an ambiguous zone for $0.7 > gdi < 0.2$.
269
270 *Clustering approaches and summary statistics*
271 We performed model-based as well as naive clustering analyses in order to check for congruence
272 with phylogenetic analyses, to identify intraspecific genetic structure, and to perform an initial
273 exploration of gene flow or admixture between species. Clustering analyses were performed
274 using corresponding methods based on ANGSD genotype likelihoods [clustering in NgsAdmix
275 v32 (Skotte et al. 2013) and PCA in ngsTools va4d338d (Fumagali et al. 2013, 2014)], on
276 GATK-called genotypes (ADMIXTURE v1.3.0; Alexander et al. 2009) and glPca (adegenet
277 v2.1.1; Jombart 2008; Jombart and Ahmed 2011). These analyses were run separately for all

successfully sequenced samples for the five focal taxa (Tab. S1) and for a subset comprising only individuals from *M. macarthurii* and *M.* sp. #3. Heterozygosity and F_{ST} were estimated with the R packages adegenet v2.1.1 (Jombart 2008) and hierfstat (Goudet 2005) on variable sites inferred from ANGSD for comparison with clustering results.

Morphometric analyses

We measured 13 different morphometric parameters (ear length, ear width, head length, head width, snout length, inter- and intra-orbital distance, lower leg length, hind foot length, third toe length, tail length, body length and body mass) according to Hafen et al. (1998) and Zimmermann et al. (1998). Individuals were assigned to their respective taxon based on phylogenetic and clustering analyses. The morphological data of all captured and released adult mouse lemurs were compared among species and with data sets available from geographically neighboring species (Fig. 1). A linear discriminant analysis (LDA) was conducted to test for species differentiation based on morphometrics using the "MASS" R package (v7.3-51.3; Venables and Ripley 2002). Model fit was evaluated by a jackknife cross-validation and Wilks' Lambda was computed to evaluate the LDA model. R^2 values were calculated using the "flipMultivariates" package (Displayr 2018) to document the proportion of variance per parameter that is explained by the species. Quantitative morphometric comparisons between taxa were performed for all measurements with a one-way ANOVA and a post hoc Tukey test. Assumptions of the respective tests were examined using Shapiro-Wilk and Levene's tests in the R package car v3.0-2 (Fox and Weisberg 2011) beforehand.

One limitation to the morphometric analyses is that body measurements of the different taxa were obtained by at least four researchers across the five different lineages, and it cannot be ruled out

that researchers may have differed slightly in how they applied the calipers. However, the same researcher contributed data points to more than one species in at least two cases (DS, DWR).

Inference of interspecific gene flow

The D-statistic and related formal statistics for admixture make use of phylogenetic invariants to infer post-divergence gene flow between non-sister populations or taxa. However, it is important to note that the D-statistic may also be influenced by ancient population structure and should thus be interpreted with care (Eriksson and Manica, 2012; Chikhi et al., 2018). We used admixtools v4.1 (Patterson et al. 2012) to compute four-taxon D-statistics (qpDstat program), which tests for gene flow between P3 and either P1 or P2 given the topology (((P1, P2), P3), P4). In order to test for gene flow between *M. macarthurii* and *M.* sp. #3, we separately treated (1) the two distinct *M.* sp. #3 population groups detected by clustering approaches, and (2) *M. macarthurii* individuals with and without "*M.* sp. #3-type" mtDNA (see Results). We also used all possible configurations in which gene flow between non-sister species among the five ingroup species could be evaluated. In all tests, *M. murinus* was used as P4 (outgroup). Significance of D-values was determined using the default Z-value reported by qpDstat, which is determined by weighted block jackknifing and is conservative for RADseq data given that linkage disequilibrium (LD) is, on average, expected to be lower across a pair of RADseq SNPs than across a pair of SNPs derived from whole-genome sequencing (Patterson et al. 2012; Kim et al. 2018).

G-PhoCS v1.3 (Gronau et al. 2011), a Bayesian MSC approach that incorporates introgression, was used to jointly infer divergence times, population sizes, and rates of gene flow between specific lineages. Because running G-PhoCS for all individuals was not computationally feasible, we performed separate runs for two sets of individuals: (1) a 3-species (and 12-individual) data

set with six *M.* sp. #3, three *M. macarthurii*, and three *M. lehilahytsara* individuals, wherein *M.* sp. #3 was divided into the two distinct population clusters detected using clustering approaches; and (2) the 5-species (and 12-individual) data set used for SNAPP and BPP. Details of the inference of gene flow are described in the Supplementary Material.

Estimation of divergence times

We used two approaches to estimate divergence times under the MSC model: (1) BPP v4.0.4 (Flouri et al. 2018), which assumes no migration after the onset of divergence, and (2) G-PhoCS, which can accommodate migration between specific lineages and co-estimate migration rates and divergence times.

Both BPP and G-PhoCS analyses used full-length RAD loci from the 12-individual dataset. The species tree recovered from phylogenetic analyses was fixed for parameter sampling. We required at least one individual per species to be present for each locus (on a total of 17,422 RAD loci) and all individuals were treated as unphased diploid sequences. We used diffuse priors, multiple chains, and checked for convergence (Supplementary Material). We also compared posteriors to marginal priors to check that parameter estimates were informed by the RADseq data and not only the priors.

Inference of effective population sizes through time

A number of studies have shown that population structure can generate spurious signals of population size change (Beaumont, 2004; Chikhi et al., 2010; Heller et al., 2013). For example, sequentially Markovian coalescent approaches such as MSMC accurately which is only equivalent to an effective size in panmictic models (Mazet et al., 2016; Rodriguez et al. 2018).

We therefore inferred and compared population size histories using several methods for the focal species *M.* sp. #3, for which we had whole-genome sequence data in addition to the RADseq data. For all species, we examined changes in N_e over time based on θ estimates from BPP and G-PhoCS for each predefined extant or ancestral population, which also allowed us to evaluate uncertainty in population size estimates due to migration. For *M.* sp. #3, we also estimated N_e over time with the Sequential Markovian Coalescent as implemented in MSMC (Schiffels and Durbin 2014) using the whole-genome data. A detailed description for these analyses is given in the Supplementary Material.

Results

RADseq data and *M.* sp. #3 genome sequence

This study demonstrates the utility of cross-laboratory RAD sequencing for primates, as previously shown in other taxa (e.g., Gonen et al. 2015). We used three different library generation protocols, two sequencing lengths, and a combination of single and paired-end sequencing, yielding highly compatible data for all 65 individuals included in the study. From more than 447 million raw reads (Tab. S1), over 394 million passed quality filters with approximately 182 million successfully aligned to the *M.* sp. #3 reference genome. There was an average of 120,000 loci per individual with coverage ranging from ~1 to ~22x (Tab. S1).

We assembled approximately 2.5 Gb of nuclear genome sequence data for *M.* sp. #3 with a contig N50 around 36 Kb (Tab. S2). While the final assembly was fragmented, as expected for a single Illumina library genome, only 6.4% of mammalian BUSCOs were found to be missing. Annotation statistics were largely comparable to BUSCO analysis of the genome assembly. The genome sequence and associated gene annotations can be accessed through NCBI (Bioproject PRJNA512515).

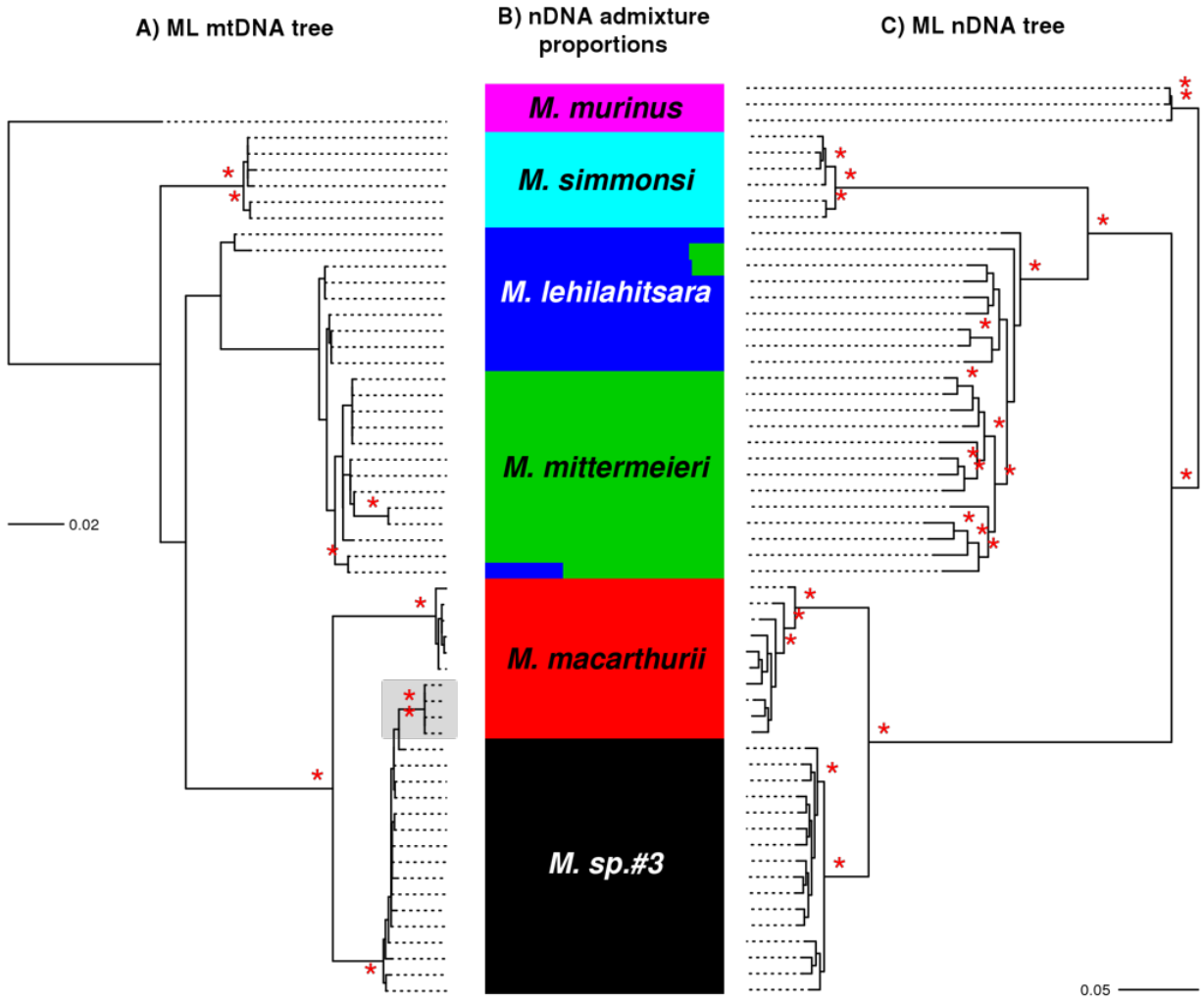

374

375 **Figure 2: Phylogenetic relationships and ancestry proportions**

376 **(A)** Maximum-likelihood RAxML tree of 55 samples represented by 4,060 bp of mtDNA recovered from
377 RADseq and Sanger sequencing (Table S1). The gray shaded box highlights individuals of *M. macarthurii*
378 with *M.* sp. #3 mtDNA haplotypes. **(B)** Clustering results using NgsAdmix at $K = 6$. **(C)** Maximum-
379 likelihood RAXML tree obtained using RADseq nuclear data (nDNA). For all trees, *M. murinus* is used as
380 the outgroup. In **(A)** and **(C)**, bootstrap support values >90% are indicated above each node as a red
381 asterisk.

382 **Phylogenetic relationships**

383 Five divergent lineages (*M. simmonsi, M. lehilahytsara, M. mittermeieri, M. macarthurii, M.* sp.
384 #3) were confirmed to occur in the study region by phylogenetic approaches (Fig. 2). One
385 lineage*, M.* sp. #3, is described here as new to science (see *Species Description*).
386
387 RAxML, SVDquartets, and SNAPP analyses recovered well-supported monophyletic nDNA
388 clades for *M. simmonsi*, *M. macarthurii*, and *M.* sp. #3 (Fig. 2; Fig. S1; Fig. S2), with
389 *M.* sp. #3 as sister to *M. macarthurii* with 100% bootstrap support (RAxML and SVDquartets,
390 Fig. 2; Fig. S2). In contrast, *M. lehilahytsara* and *M. mittermeieri* were not consistently
391 monophyletic in RAxML analyses of nDNA (Fig. 2C) or mtDNA (Fig. 2A), both of which
392 nested *M. mittermeieri* within *M. lehilahytsara*. SVDquartets analysis of nDNA placed an
393 individual from Ambavala (B12) as sister to all other *M. lehilahytsara* and *M. mittermeieri* with
394 weak bootstrap support (Fig. S2A). Unsurprisingly, species tree analyses with SNAPP (the 22-
395 individual dataset included B12 from Ambavala) recovered *M. lehilahytsara* as sister to *M.*
396 *mittermeieri* with no topological uncertainty (Fig. S1).
397
398 One case of mitonuclear discordance was found. Although mtDNA analyses placed several
399 individuals from Anjiahely (see Fig. 1) in a well-supported clade with *M.* sp. #3 individuals from
400 Ambavala, Mananara-Nord NP and Antanambe (Fig. 2A; see lower red box), analyses of the
401 nuclear RADseq data placed them unambiguously within the *M. macarthurii* clade (Fig.
402 2B,C). This suggests that individuals from Anjiahely belong to *M. macarthurii* yet carry two
403 divergent mtDNA lineages, and that *M.* sp. #3 is only found from Ambavala to Antanambe
404 (Fig. 1). The cause of potential mitonuclear discordance for *M. macarthurii* in Anjiahely was
405 subject to further investigation (see below in the section “Interspecific Gene Flow”).

406

407 **Species delimitation**

408 *Genetic structure*

409 Clustering analyses (NgsAdmix and ADMIXTURE) at K = 5 grouped individuals into the five
410 nominal species in accordance with phylogenetic results and F_{ST} estimates (Fig. S3; Fig.
411 S4; Tab. S3), although some individuals were inferred to have ancestry from both *M.*
412 *mittermeieri* and *M. lehilahytsara* (Fig. 2B). Using NgsAdmix, three or five clusters best
413 explained the data (Fig. S3; Fig. S5), while using ADMIXTURE, three clusters had a
414 slightly lower cross-validation error than five (Fig. S5). PCA readily distinguished all species
415 (including the two sister species *M.* sp. #3 and *M. macarthurii*) across the first four principal
416 components with both GATK genotypes (Fig. 3A,B) and ANGSD genotype likelihoods
417 (Fig. S7).

418

419 When restricting clustering analyses to *M. macarthurii* and *M.* sp. #3 individuals, K = 2 was the
420 best-supported number of clusters using both approaches (Fig. S5; Fig. S6), which
421 divided *M. macarthurii* and *M.* sp. #3 individuals into separate clusters. At K = 3, *M.* sp. #3 was
422 split into two clusters individuals from Mananara-Nord NP and Antanambe on one hand and
423 individuals from Ambavala on the other (Fig. S8). PCA analyses for this subset of individuals
424 clearly distinguished these two groups along PC2 (Fig. 3C). Hereafter, we refer to these two
425 groups as "southern *M.* sp. #3" (Mananara-Nord NP and Antanambe, which is south of the large
426 Mananara river) and "northern *M.* sp. #3" (Ambavala, which is north of the river; Fig. 1).

427

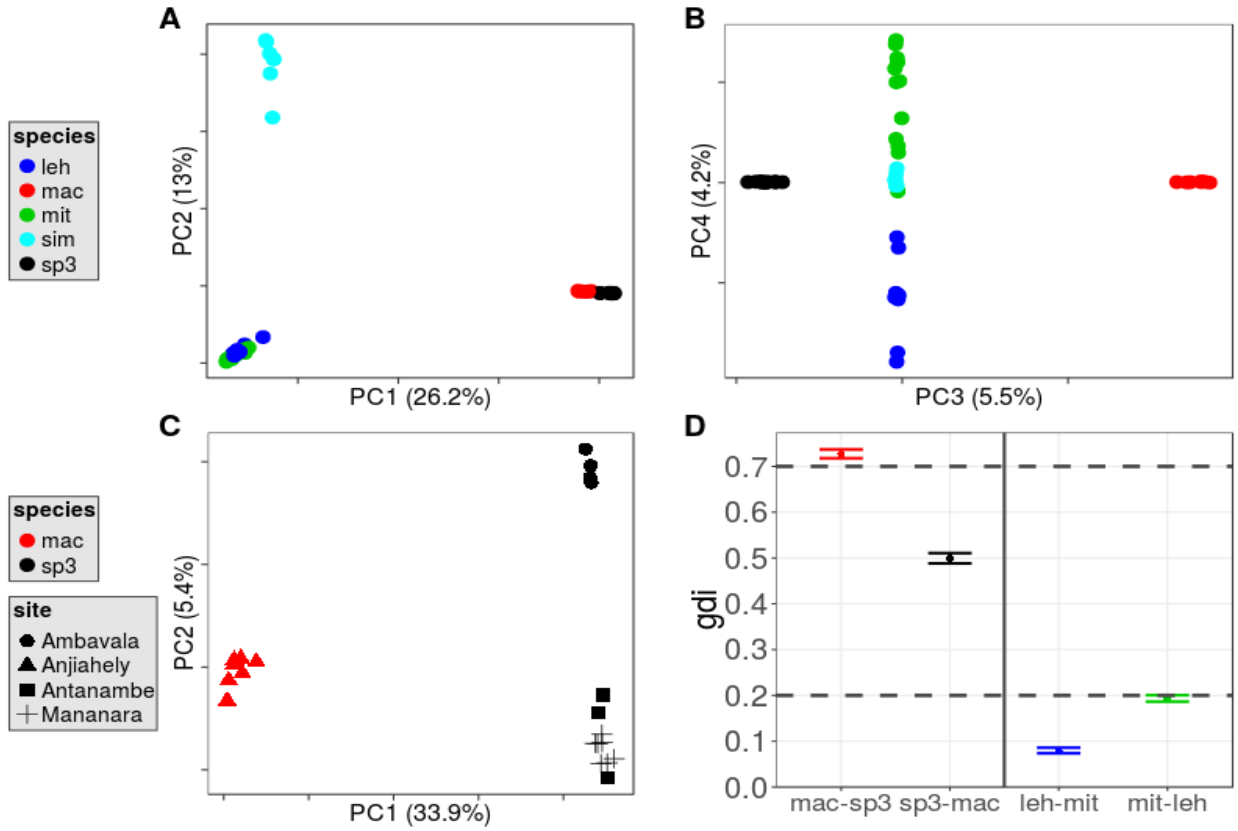

Figure 3: Population genetic structure and the *gdi*.

PCA analyses for **(A, B)** all five species and **(C)** restricted to *M.* sp. #3 and *M. macarthurii* individuals, the latter showing the split of the two population groups "northern" (Ambavala) and "southern" *M.* sp. #3 (Antanambe and Mananara-Nord NP). **(D)** Genealogical divergence index (*gdi*) for *M. macarthurii* – *M.* sp. #3 and *M. mittermeieri* – *M. lehilahytsara*. *gdi* values > 0.7 suggest separate species; *gdi* values < 0.2 are below the lower threshold for species delimitation; 0.2 < *gdi* < 0.7 are in an "ambiguous" range (Jackson et al. 2017). Abbreviations: leh: *M. lehilahytsara*, mac: *M. macarthurii*, mit: *M. mittermeieri*, sim: *M. simmonsi*, sp3: *M.* sp. #3.

428 *SNAPP Bayes Factors*

429 Bayes factors strongly favored splitting *M.* sp. #3 and *M. macarthurii* into two separate species in

430 the 22-individual analyses (2lnBF = 34,326.39, `Tab. 1`). This indicates that levels of gene flow

431 between *M.* sp. #3 and *M. macarthurii* are low, considering that one migrant per generation

between species can erode evidence for species assignment under the MSC (Zhang et al. 2011). Bayes factors for the 22-individual dataset also supported splitting *M. lehilahytsara* and *M. mittermeieri*, albeit with much weaker support than the *M.* sp. #3 and *M. macarthurii* split (2lnBF = 993.06). All species assignments were also recovered by the guided delimitation analysis (Fig. S9).

Table 1: Bayes factor support for sister species pairs.

Marginal likelihoods were computed for a hypothesis of no speciation (Merge) and a hypothesis of a speciation event (Split). We tested both the *M.* sp. #3 - *M. macarthurii* lineages and *M. lehilahytsara* - *M. mittermeieri* species pairs with a 12- and 22-individual dataset. †Bayes factors calculated as 2 * (lnL_{Split} - lnL_{Merge}).

Species Pair	Number of Individuals	Merge Marginal lnL	Split Marginal lnL	2ln Bayes factor†
M. macarthurii - *M. sp. #3*	12	-134254.14	-125601.69	17304.91
	22	-204540.32	-187377.12	34326.39
M. lehilahytsara - *M. mittermeieri*	12	-126515.89	-125601.69	1828.41
	22	-187873.65	-187377.12	993.06

Genealogical divergence index (gdi)

For the *M.* sp. #3 - *M. macarthurii* sister pair, *gdi* was 0.727 (95% HPD: 0.718-0.737) from the perspective of *M. macarthurii* (i.e. above the upper threshold for species delimitation), and 0.500 (0.488-0.511) from the perspective of *M.* sp. #3 (i.e. in the upper ambiguous zone for species delimitation; Fig. 3D). In contrast, *gdi* values for the *M. lehilahytsara* - *M. mittermeieri* species pair were much lower and even below the lower threshold for species delimitation: 0.080 (0.074-0.086) from the perspective of *M. lehilahytsara*, and 0.193 (0.187-0.201) from the perspective of *M. mittermeieri* (Fig. 3D).

453 *Morphometric comparisons*

454 Though morphological distinctions are subtle, *Microcebus* sp. #3, *M. macarthurii*, *M. simmonsi*
455 and *M. mittermeieri* can be statistically distinguished based on morphometrics (LDA: Wilks'
456 Lambda = 0.0175, F = 6.7941, P < 0.001; Fig. 4). Apart from ear length, all parameters
457 contributed significantly to species assignments in the LDA model (P < 0.001), with body length
458 and inter-orbital distance having the highest R^2-values (Fig. 4, Tab. S4). Prediction
459 accuracy of the jackknife cross-validated LDA model was 81%. Mis-classifications occurred with
460 *M. simmonsi*, but not between the other three taxa (Tab. S5). All three linear discriminant
461 functions were statistically significant of which the first (LD1) explained 69.3% of interspecific
462 variation and LD2 and LD3 the remaining 23.7% and 7.0%, respectively. *M*. sp. #3 and *M.*
463 *macarthurii* predominantly differed in five "head-associated" parameters (head width, inter- and
464 intra-orbital distance, snout length, ear width, all larger in *M*. sp. #3) while limb proportions did
465 not show significant differences (Fig. 4).
466
467 Two out of three *M. macarthurii* individuals with mitonuclear discordance clustered
468 morphometrically with the other *M. macarthurii,* whereas the third was positioned with *M.*
469 *simmonsi* (Fig. 4).

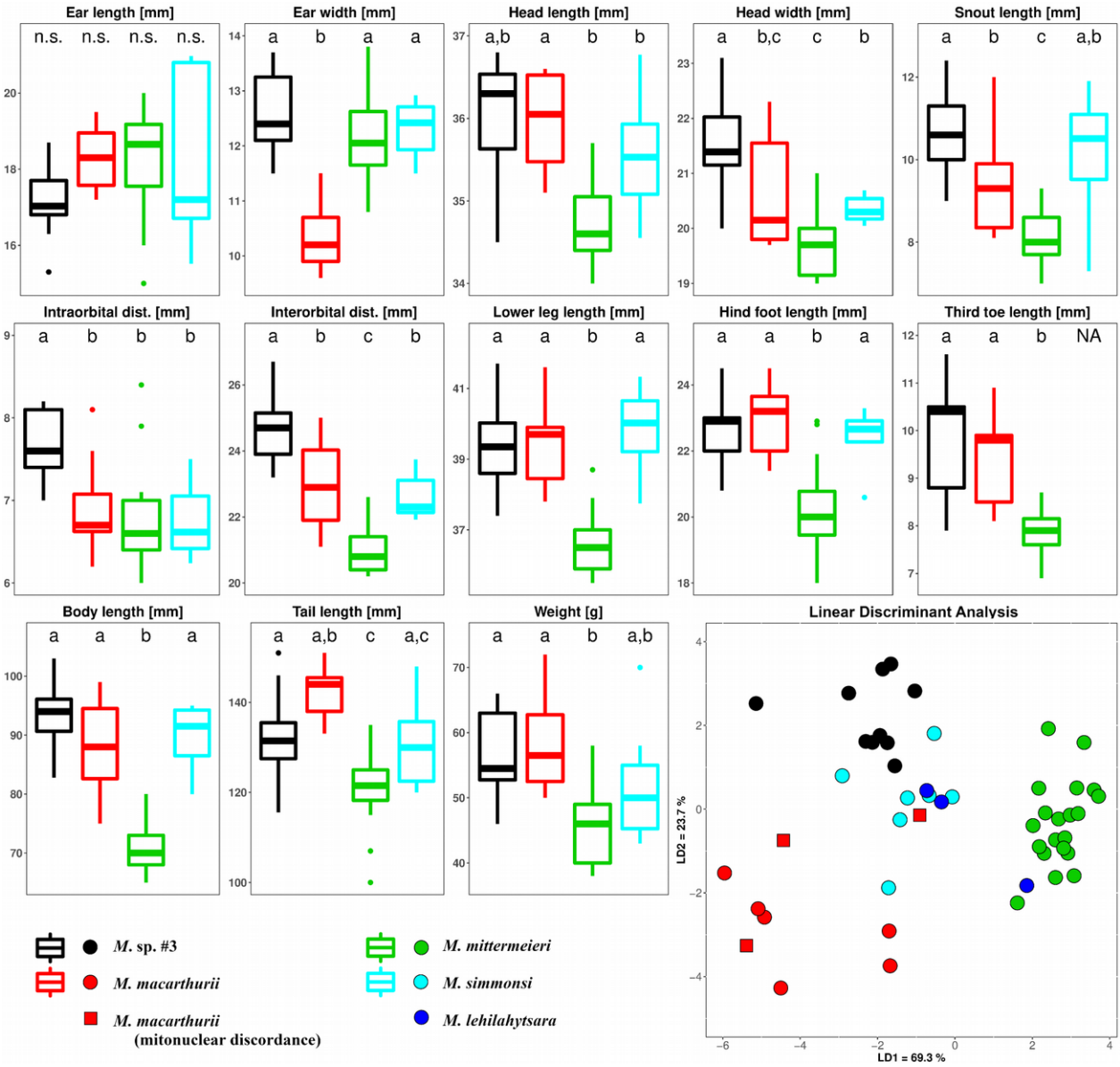

Figure 4: **Interspecific differences in morphometric parameters.**

Small plots: Comparisons based on one-way ANOVA ($P < 0.001$ for all parameters except ear length) and grouping (letters after values) according to Tukey post-hoc tests. For parameter values, see Table S4. Large plot in bottom right: Linear discriminant analysis (LDA) based on morphometric measurements (M. sp. #3, n = 11; *M. macarthurii*, n = 6; *M. mittermeieri*, n = 22; *M. simmonsi*, n = 7). Individuals of *M. macarthurii* with mitonuclear discordance and of *M. lehilahytsara* were not used to calculate the LDA model due to small sample sizes, their position was predicted using the LDA model (*M. macarthurii*, n = 3; *M. lehilahytsara*, n = 3).

Interspecific gene flow

D-statistics suggested that northern *M.* sp. #3 and *M. macarthurii* share a slight excess of derived alleles in relation to southern *M*. sp. #3, significantly deviating from 0 for the comparison inferring gene flow between northern *M*. sp. #3 and *M. macarthurii* with "*M. sp. #3*-type" mtDNA (Fig. 5A). Using a G-PhoCS model with separate northern and southern *M*. sp. #3 population groups, we found asymmetric gene flow between *M*. sp. #3 and *M. macarthurii*, and additionally inferred that (1) gene flow with *M. macarthurii* took place before as well as after the onset of divergence between northern and southern *M.* sp. #3, (2) gene flow between extant lineages occurs only between northern (and not southern) *M.* sp. #3 and *M. macarthurii* and (3) gene flow is asymmetric, predominantly into *M. macarthurii* (Fig. 5B). In a G-PhoCS model with all species, we additionally inferred gene flow from *M. mittermeieri* to *M. lehilahytsara* at higher levels than that from *M.* sp. #3 to *M. macarthurii* (*Fig. 6A*).

Low levels of gene flow were also inferred between the *M.* sp. #3 - *M. macarthurii* clade and the *M. mittermeieri* - *M. lehilahytsara* clade, most likely between ancestral populations but the timing and direction of gene flow could not be determined in more detail (Supplementary Results; Fig. S10).

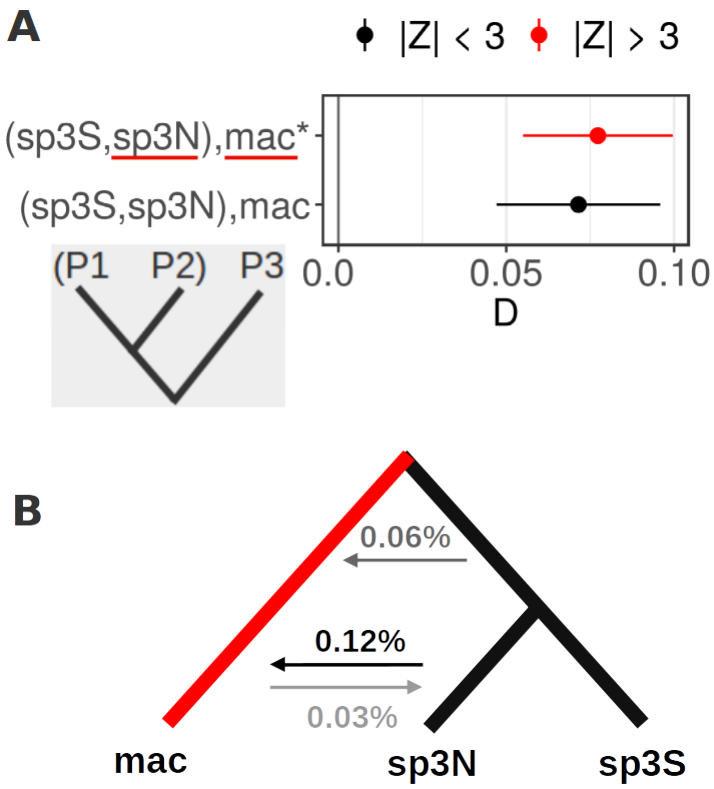

Figure 5: Gene flow between *M.* sp. #3 and *M. macarthurii*.

(A) Four-taxon D-statistic suggesting gene flow between *M. macarthurii* ("mac") and northern *M.* sp. #3 ("sp3N"). In the lower comparison, *M. macarthurii* individuals with mitonuclear discordance ("mac*"), are treated separately. Axis annotations denote "(P1,P2),P3", wherein gene flow is tested between P3 and either P1 (negative D) or P2 (positive D). The outgroup P4 was *M. murinus* for all tests. Significant comparisons (|Z| > 3) are in red. **(B)** Percentage of migrants in each generation, inferred by G-PhoCS under a model with three taxa: *M. macarthurii* sister to northern and southern *M.* sp. #3. Shade of gray of arrows and text reflect the relative amount of gene flow.

Divergence Times

We estimated divergence times using the MSC model with BPP as well as G-PhoCS with and without interspecific gene flow (Fig. 6; Fig. S11). Results were similar across these approaches, although divergence times were estimated to be older in G-PhoCS models with migration compared to models without migration (Fig. 6). Specifically, the divergence time of *M*. sp. #3 and its sister taxon *M. macarthurii* was estimated at 50-109 kya (min. max. of 95% HPD across all models) without migration (Fig. 6; Fig. S11), but at 91-183 kya when incorporating gene flow between the two (Fig. 6). The effect of accounting for gene flow was particularly strong for divergence times between *M. mittermeieri* and *M. lehilahytsara* (Fig. 6): while the estimated divergence time of *M. mittermeieri* and *M. lehilahytsara* without gene flow was highly similar to that between *M.* sp. #3 and *M. macarthurii* (50-97 kya; Fig. 6), it was estimated to be 250-478 kya in the presence of migration (Fig. 6). Ages of other nodes were not affected strongly by including migration into the MSC model. For example, the split between the last common ancestor of *M.* sp. #3 / *M. macarthurii* and the last common ancestor of *M. mittermeieri* / *M. lehilahytsara* / *M. simmonsi* was estimated to be 351-756 kya when not accounting for gene flow, and 348-648 kya when accounting for gene flow (Fig. 6D). These posterior estimates are likely not influenced strongly by the model priors based on comparison of marginal priors and posteriors across four BPP chains (Fig. S12).

Population sizes through time

Effective population sizes for extant as well as ancestral lineages were first estimated using BPP and G-PhoCS (with and without interspecific gene flow; Fig. 6A-C). We found large differences among species, with considerably larger effective population sizes for *M. murinus* (min. and max. 95% HPD across the BPP and both G-PhoCS models: 59-79 k), *M. lehilahytsara*

(63-139 k), *M. mittermeieri* (42-86 kya), and most ancestral lineages, than for *M.* sp. #3 (14-20 k), *M. macarthurii* (6-10 k), and *M. simmonsi* (19-26 k). Wide HPD intervals for *M. mittermeieri* and *M. lehilahytsara* were due to differences between models that did and did not account for gene flow between these two species. Using the 3-species G-PhoCS model, effective population sizes were estimated separately for northern (14-41 k), southern (7-20 k), and ancestral (18-31 k) *M.* sp. #3 lineages (Fig. S10). An MSMC analysis for a single *M.* sp. #3 individual belonging to the southern group resulted in highly similar estimates of population sizes through time, showing a marked long-term decline towards the present (Fig. 6F). The estimated differences in recent effective population sizes across taxa were further reflected by differences in genetic diversity across populations (Fig. S13).

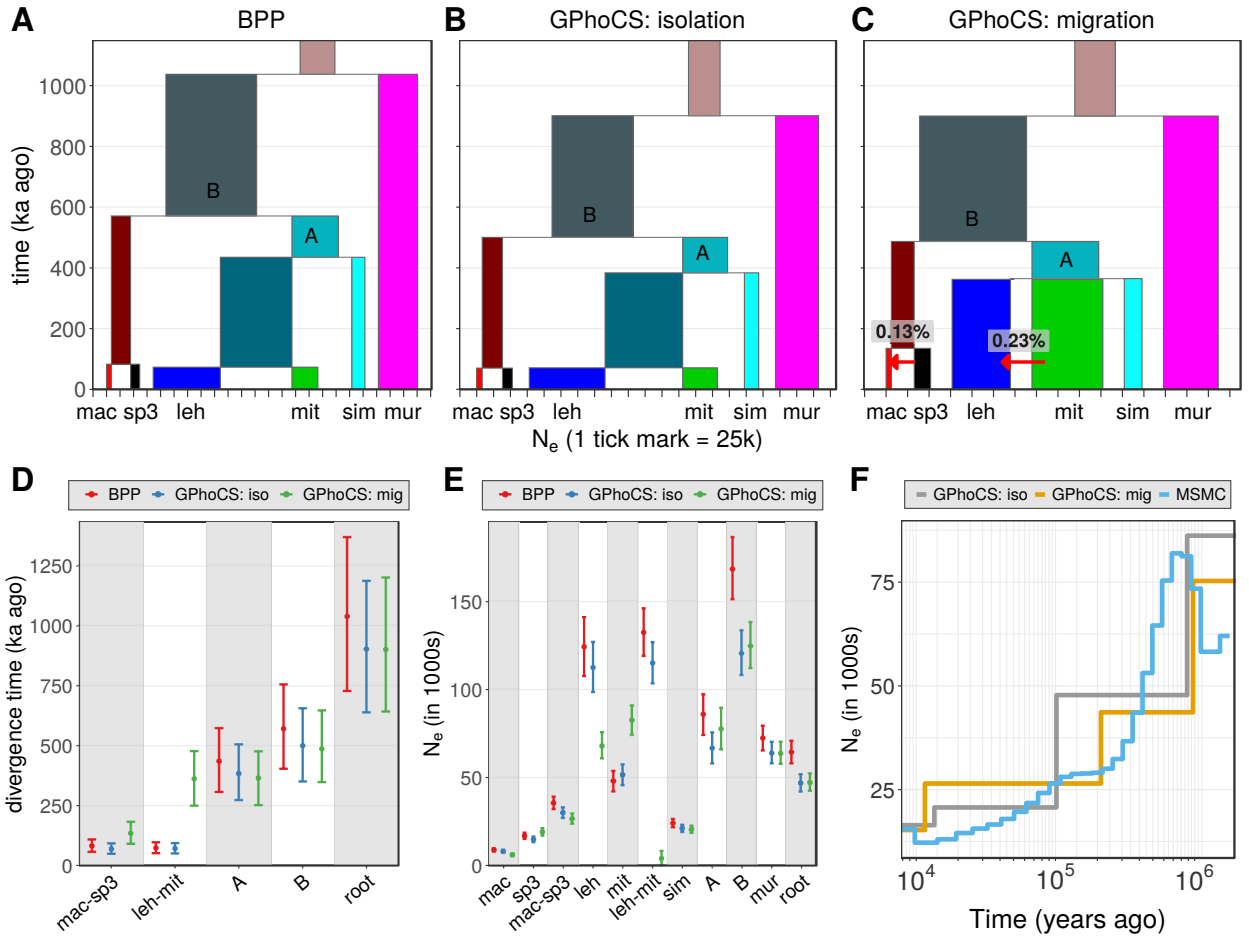

538

539 **Figure 6: Demographic histories inferred by G-PhoCS, BPP and MSMC.**

540 **(A-C)** Divergence times (y-axis) and effective population sizes (x-axis) inferred with and without migration.

541 **(D, E)** Comparison of divergence times and effective population sizes for each node and lineage,

542 respectively. “A” represents the lineage ancestral to *M. simmonsi*, *M. mittermeieri* and *M. lehilahytsara*, “B”

543 represents the lineage ancestral to *M.* sp. #3, *M. macarthurii*, *M. simmonsi*, *M. mittermeieri* and *M.*

544 *lehilahytsara*, and *“root”* represents the lineage ancestral to all six species included. **(F)** Effective

545 population sizes through time for *M.* sp. #3 as inferred by MSMC for whole-genome data from a single

546 individual (blue line), and by G-PhoCS for RADseq data for individuals from the same population group

547 (southern *M. sp. #3*) in the 3-species model, with and without gene flow (yellow and gray lines,

548 respectively).

Discussion

The results of this study document rapid lineage diversification of mouse lemurs within a restricted region in Madagascar. Even though the species from the study region all diverged from their common ancestors within the past 500,000 years, two pairs of non-sister species occur sympatrically. Evidence supporting the divergent species identity of *M. jonahi* and its sister species *M. macarthurii* is much stronger than for a previously described species pair. Furthermore, a comparison of MSC models with and without gene flow produced different divergence age estimates and showed that differences in effective population size appear to have consequences for species delimitation.

Strong support for *M.* sp. #3 as a separate species: *M. jonahi*

Evidence for distinguishing *M.* sp. #3 as a separate species from *M. macarthurii* was strong and consistent across a variety of species delimitation approaches. The two lineages were found to be reciprocally monophyletic across all phylogenetic analyses of RADseq data (Fig. 2C; Fig. S1; Fig. S2), separated unambiguously in clustering analyses (Fig. 2B; Fig. 3; Fig. S3; Fig. S5–S7), had strong support for two separate species from SNAPP Bayes factors (Tab. 1) and BPP (Fig. S9), and passed the heuristic criterion of *gdi* (Fig. 3D). Nevertheless, these two lineages have diverged from each other relatively recently, with median estimates of the divergence time across three different models with and without gene flow all under 100 kya. While recent, it is important to keep in mind that if we were to transpose the number of generations in this divergence time to a "hominin scale" (with a generation time that is seven to ten times longer than that of mouse lemurs), this would correspond to a period longer than 500,000 years, close to the estimated divergence time between Neanderthals and *Homo sapiens*.

573

574 Though subtle, morphological evidence also supported the distinctiveness of *M.* sp. #3 in
575 comparison to all other species that occurred in the same biogeographic region (Fig. 4). *M.* sp.
576 #3 is differentiated from its sister species *M. macarthurii* in five out of 13 measured
577 morphometric parameters. Differences between the two sister taxa predominantly appeared in
578 head-associated parameters such as ear and head width, orbital distances, and snout length. It has
579 been suggested that skull parameters vary with feeding habits in lemurs and strepsirrhine
580 primates in general (e.g., omnivorous, folivorous or frugivorous etc.; Viguier 2004; Meloro et al.
581 2015; Fabre et al. 2018). We hypothesize that the morphometric differences in head-associated
582 parameters may indicate dietary and possibly cognitive differentiation between these two sister
583 species (Zimmermann and Radespiel 2014). Based on these signatures of genomic and
584 morphological distinctiveness, species status is supported for *M.* sp. #3 and a full species
585 description using the name *M. jonahi* is given at the end of the manuscript.

586

587 **Signatures of gene flow between a recently diverged sister species pair**

588 Mitonuclear discordance was observed for a subset of *M. macarthurii* individuals from
589 Anjiahely. Though having nDNA indistinguishable from other *M. macarthurii* at the same site,
590 across phylogenetic and clustering analyses, these individuals carried mtDNA similar to that of
591 *M.* sp. #3 (see Radespiel et al. 2008). And though genealogical discordance is not unexpected due
592 to incomplete lineage sorting, the strength and direction of the disagreement suggests
593 mitochondrial introgression, which was supported by D-statistics (Fig. 5A) and the inference
594 of low levels of gene flow from the *M.* sp. #3 population north of the Mananara river into *M.*
595 *macarthurii* by G-PhoCS (Fig. 5B). Therefore, the discovery of a divergent mtDNA lineage at
596 Anjiahely (Radespiel et al. 2008; Fig. 1), which prompted the current work and led to the

discovery of a new species, appears to have been the result of local mtDNA introgression into its sister species.

The roles of population size and gene flow in species delimitation

In contrast to *M.* sp. #3 and *M. macarthurii*, we found only weak support for separate species status of *M. lehilahytsara* and *M. mittermeieri*. They showed paraphyly in ML and SVDquartets analyses (Fig. 2A,C; Fig. S2), were not as clearly separated in clustering analyses (Fig. 2B; Fig. S3; S5; Fig. S6), and had weak Bayes factor support in SNAPP relative to *M.* sp. #3 and *M. macarthurii* (Tab. 1). Most strikingly, reciprocal *gdi* statistics were below the recommended lower range for diagnosing species status (Jackson et al. 2017; Leaché et al. 2019; Fig. 3D). We must therefore remain open to the possibility that boundaries between previously described species may be revealed as ambiguous in light of new methods and results. The methods used here thus do not necessarily lead to ever-increasing numbers of species, but rather offer a reasonable way forward in our effort to accurately delimit biodiversity. And, when coupled with other population genomic approaches, these methods offer insight into the complex demographic history of diverging populations that may be in the process of speciation.

Even so, it should be emphasized, that most of the disparities in levels of support for species status between the two pairs of sister species may be a fundamental consequence of differences in effective population sizes, which are much larger for the *M. mittermeieri* / *M. lehilahytsara* pair than for the *M.* sp. #3 / *M. macarthurii* pair. The *gdi* is calculated using the population sizes and divergence times that are estimated without accounting for potential gene flow. Since those divergence time estimates are highly similar for both species pairs, the difference in *gdi* is largely the result of differences in effective population sizes. This is expected, since larger effective

621 population sizes result in slower sorting of ancestral polymorphisms (Maddison 1997), and the
622 *gdi* relies on quantifying the probability that two sequences from the focal taxon coalesce more
623 recently than the divergence time between the taxa. More generally, differences in population
624 sizes may also explain why *M. mittermeieri* and *M. lehilahytsara* were not resolved as clades in
625 the nDNA phylogeny (Fig. 2C) yet are shown to have distinct genetic clusters (Fig. 2B;
626 Fig. 3B).
627
628 Assessing speciation completion by quantifying rates of neutral coalescence is based on the
629 assumption that the magnitude of genetic drift is a good predictor of progress in speciation. This
630 is problematic, however, given that the role of drift in speciation is generally thought to be small
631 (Rice and Hostert 1993; Coyne and Orr 2004; Czekanski-Moir and Rundell 2019; but see Uyeda
632 et al. 2009), and a high prevalence of gene flow during and after speciation (Feder et al. 2012;
633 Harrison and Larson 2014; Mallet et al. 2016; Campbell et al. 2018) may restrict the build-up of
634 neutral differentiation, even over longer time spans. Moreover, the possibility that progress in
635 speciation is decoupled from neutral genetic differentiation cannot be avoided when delimiting
636 species using molecular data (Guilot et al. 2012; Solis-Lemus et al. 2015). Nevertheless, a
637 reliance on genealogical divergence in coalescence-based species delimitation specifically
638 renders effective population size a key variable. It is not clear whether this is justified, and
639 additional measures of divergence that do not depend on effective population sizes may also need
640 to be considered (see also Hey and Pinho 2012; Martien et al. 2017 – Appendix 2). Thus far, few
641 studies have examined a potential link between effective population size and speciation rates
642 (Khatri and Goldstein 2015; Khatri and Goldstein 2018; Huang et al. 2018), especially outside of
643 the context of founder effect speciation (Mayr 1959; Boake and Gavrilets 1998; Matute 2013).
644

A further distinction between the two pairs of sister species examined by this study is that we find higher rates of gene flow between *M. mittermeieri* and *M. lehilahytsara* (Fig. 6A). This is not simply a consequence of overall lower differentiation, since divergence time is estimated to be substantially older than that of *M.* sp. #3 / *M. macarthurii* when accounting for gene flow within both species pairs. Thus, a joint consideration of genealogical divergence and rates of gene flow may offer a way forward for effective and consistent genomic species delimitation (see also Hey and Pinho 2012) with our study showing that this is an area ripe for future exploration.

Rapid speciation in mouse lemurs

Sympatric *Microcebus* species were found at two study sites: *M. macarthurii* and *M. mittermeieri* in Anjiahely (Makira) and *M.* sp. #3 and *M. lehilahytsara* in Ambavala (Fig. 1). This is remarkable given that until now, only four other cases of sympatry among mouse lemur species are known, and in all cases with only two species co-occurring, and always with *M. murinus* as the other resident (Radespiel 2016). Moreover, the two sympatric pairs of species in this study were estimated to have a common ancestor only ~500-600 kya. This provides strong evidence that mouse lemurs not only developed widespread and rapid genetic divergence among geographic areas, but also rapid reproductive isolation. Assuming that the geographic mode of speciation has been largely allopatric (which is e.g. supported by the allopatric distributions of sister species in this study), the observed sympatry of two pairs of non-sister species also reveals substantial dynamism in the ranges of at least some of the focal species. It is tempting to speculate that secondary contact occurred due to range expansion of *M. mittermeieri* and *M. lehilahytsara*, which have larger ranges and population sizes as well as higher levels of interspecific gene flow than the decreasing micro-endemics *M. sp. #3* and *M. macarthurii*.

669 Coalescent-based estimates of divergence times constrain the speciation of the focal lineages to
670 the Pleistocene (<600,000 years). It is therefore plausible that past climatic oscillations,
671 especially periods of drought accompanied with turnovers in vegetation composition and the
672 contraction of forested habitats were a factor in the isolation and genetic divergence of the
673 sampled species and populations (Burney et al. 1997; Gasse and Van Campo 2001; Kiage and
674 Liu 2006; Wilmé et al. 2006). In addition, the Mananara river appears to have impacted
675 population structure within *M*. sp. #3 and restricted gene flow between *M*. sp. #3 and *M.*
676 *macarthurii*, emphasizing that large rivers can be phylogeographic barriers in lemurs (Martin
677 1972; Pastorini et al. 2003; Goodman and Ganzhorn 2004; Olivieri et al. 2007).
678
679 Making direct links between molecular divergence and geological time is challenging. As a case
680 in point, some estimated divergence times were sensitive to whether gene flow was accounted for
681 in the MSC model (Fig. 6). Specifically, the model incorporating gene flow between *M.*
682 *lehilahytsara* and *M. mittermeieri* shifted their divergence time backwards by nearly 300 kya,
683 though estimates for deeper nodes were not similarly affected. The substantial effect of
684 incorporating or disregarding gene flow on divergence time estimation has been previously noted
685 (Leaché et al. 2014) and we here reiterate its importance for future studies. Furthermore,
686 development and application of methods that co-estimate divergence and gene flow for large-
687 scale genomic data, such as recent MSC methods that model introgression with phylogenetic
688 networks that are capable of marginal likelihood estimation (Zhang et al. 2017), will be crucial
689 for the accurate characterization of speciation processes.
690
691 A notable feature of the coalescent-based estimates of divergence times presented here is that
692 they are drastically different compared to those derived from fossil-calibrated molecular clock

693 methods. The basal divergence between *M. murinus* and the focal five-species clade in this study
694 was estimated to be close to 1 mya, but has consistently been estimated to be approximately 8 -
695 10 mya using fossil-calibrated estimates (Yang and Yoder 2003; dos Reis et al. 2018). Several
696 factors may explain this difference. First, we used a recent pedigree-based estimate of the mouse
697 lemur mutation rate that is about 2.5-fold higher than the phylogenetically-based estimate for
698 mouse lemurs (Campbell et al. 2019). Second, concatenated and gene tree-based estimates are
699 theoretically expected to overestimate recent species divergence times (Edwards and Beerli 2000,
700 Arbogast et al. 2002) and empirical comparisons have indeed found considerably more recent
701 divergence time estimates using coalescent-based estimates (McCormack et al. 2011; Angelis &
702 Dos Reis 2015; Colombo et al. 2015). Finally, fossil-calibrated estimates for lemurs require
703 external calibrations from distantly related lineages given the absolute dearth of lemur fossils
704 (e.g., Yang and Yoder 2003; Herrera and Dávalos 2016). Overall, the mouse lemur radiation is
705 likely more recent than previously suggested, yet further investigation is needed to understand the
706 magnitude of these disparate estimates.
707
708 **Endangered "hotspot for micro-endemism" in northeastern Madagascar**
709 In total, we found five evolutionarily divergent lineages of *Microcebus* within a 130 km wide
710 stretch of lowland rain forest in northeastern Madagascar making this restricted region one of the
711 most species-rich areas thus far identified for mouse lemurs. Although all taxa can be found in
712 varying habitat types (except heavily degraded grass- and fernlands), primary forests, even of
713 varying degradation stages, are strongly preferred (Knoop et al. 2018; Miller et al. 2018; Schüßler
714 et al. 2018).
715

716 A long-term decline in population size was inferred for the lineage leading to *M*. sp. #3. While
717 changes in inferred N_e may be confounded by changes in population structure, especially for
718 single-population PSMC/MSMC models that do not explicitly consider population subdivision
719 (Mazet et al., 2016, Chikhi et al., 2018), we found highly similar results between MSMC and G-
720 PhoCS analyses that considered divergence across a model with three species, treating the two *M.*
721 sp. #3 population clusters separately (Fig. 6F). This is especially reassuring since MSMC
722 analysis used whole-genome data for a single individual, while RADseq data from multiple
723 individuals per population underlies the G-PhoCS analyses. Importantly, changes in population
724 structure may also be associated with actual changes in population size, such as successive
725 population subdivision events with limited or no subsequent gene flow. If such changes in
726 population structure are the main cause of population size changes, as appears to be the case for
727 the lineage leading to *M.* sp. #3, a high degree of concordance between these different types of
728 analyses would in fact be expected. Nevertheless, we stress that future work will likely need to
729 study more complex scenarios of connectivity using metapopulation models, as has been
730 suggested for humans (Scerri et al., 2018).
731
732 The decline and population subdivision of *M*. sp. #3 was inferred to have started long before
733 anthropogenic land use fragmented the forest habitats, supporting the emerging consensus that
734 human colonization in Madagascar alone does not explain the occurrence of open habitats and
735 isolated forest fragments (Quéméré et al. 2012; Yoder et al. 2016; Vorontsova et al. 2016; Hackel
736 et al. 2018). However, we also observed clade-specific population size dynamics within the same
737 region, with *M. mittermeieri* and especially *M. lehilahytsara* maintaining much larger population
738 sizes than *M*. sp. #3 and its sister species, *M. macarthurii*, which appear to have decreased in
739 ranges and population sizes. It remains unclear what underlies these striking differences in

740 population sizes between the two pairs of sister species, which is especially mysterious given that
741 the four lineages occupy essentially the same geographic area.
742
743 Even so, the results of our study emphasize the need to intensify conservation activities in the
744 region (Schüßler et al. 2018). The exact range of *M.* sp. #3 is not yet established, but likely does
745 not exceed a maximum size of about 6,700 km². The known distribution includes community-
746 protected forests around Ambavala (Schüßler et al. 2018) and one nationally protected area with
747 Mananara-Nord NP. The southern range boundary of this species is most likely the Anove river
748 (Fig. 1), given that we detected *M. simmonsi* directly south of this river (which represents a
749 northern expansion of the known range for *M. simmonsi* that had previously been found at
750 Zahamena NP, Betampona and Tampolo; Louis et al. 2006; Louis and Lei 2016).
751
752 *M. lehilahytsara* has so far been assumed to represent a highland specialist, with no previous
753 records below 825 m a.s.l. (Weisrock et al. 2010; Radespiel et al. 2012). Unexpectedly,
754 individuals at Ambavala, at an elevation of 235 m a.s.l., were grouped together with *M.*
755 *lehilahytsara* from a highland study site (Riamalandy). This finding needs to be interpreted with
756 caution, however, due to weak overall differentiation between *M. lehilahytsara and M.*
757 *mittermeieri* and a lack of samples from intermediate locations. Thus, further research is required
758 to resolve this relationship and implications for the evolutionary history and biogeography of *M.*
759 *lehilahytsara*.
760
761 Recent analyses show that preferred forest habitats are rapidly declining and the isolation of
762 protected areas is inevitable in the foreseeable future (Schüßler et al. under review). We are now
763 beginning to appreciate that the area of northeastern Madagascar represents a “hotspot for micro-

764 endemism", while simultaneously finding that a newly described species may be under high
765 extinction risk due to ongoing deforestation (Schüßler et al. under review) and anticipated
766 environmental changes due to climate change (Brown and Yoder 2015). This situation is
767 unfortunately reminiscent of the recent discovery of *Pongo tapanuliensis*, which became the last
768 great ape species to be discovered and the most threatened at the same time (Nater et al., 2017).
769

770 ## Conclusions

771 We have used both morphometric analyses and genomic species delimitation to show that five
772 species of mouse lemurs, one of which is newly described, occur in a restricted region of
773 northeastern Madagascar, making it a hotspot for micro-endemism and conservation concern in
774 accordance with findings from Wilmé et al. (2006) and Brown and Yoder (2015). Furthermore,
775 we have shown that two pairs of non-sister species occur sympatrically despite surprisingly
776 recent estimated divergence times. From these results, we infer that speciation in mouse lemurs
777 can occur more rapidly than previously suspected, and the challenge ahead is to disentangle the
778 temporal dynamics and the geographic and ecological drivers of evolutionary diversification
779 within cryptic, young, and highly speciose radiations.
780

781 We also emphasize the need to carefully consider the potentially confounding effects of gene
782 flow and population structure when estimating divergence times and changes in effective
783 population sizes, and call for the development of metapopulation models to interpret genomic
784 data and increase our understanding of the consequences of past climatic oscillations on patterns
785 of genomic diversity and differentiation. Finally, we show that the inference of the degree to
786 which speciation has progressed in the two sister-species pairs of mouse lemurs studied here
787 correlates strongly with their respective effective population sizes. This finding suggests the need

788 for a critical evaluation of the implicit assumption in molecular species delimitation that N_e and

789 rates of drift correlate with the rate at which speciation progresses.

Species Description

Systematics

Order: Primates (Linnaeus 1758)

Suborder: Strepshirrini (É. Geoffroy 1812)

Family: Cheirogaleidae (Gray 1873)

Genus: *Microcebus* (É. Geoffrroy 1828)

Species: *Microcebus jonahi* species nova

Holotype

B34, adult male, captured on 06 September 2017 by DS. Tissue samples, hair samples as well as e-voucher photos of the animal are stored at the Institute of Zoology, University of Veterinary Medicine Hanover, Germany. The animal itself was released after field handling, sampling, and photographing, since its taxonomic distinctiveness was not recognized at the time of capture. Field measurements (all lengths measured in mm): ear length: 17.6, ear width: 13.7, head length: 37.7, head width: 23.0, snout length: 10.0, intra-orbital distance: 8.2, inter-orbital distance: 26.0, lower leg length: 41.7, hind foot length: 24.5, third toe length: 10.6, body length: 95.6, tail length: 130.0, body mass: 66 g. The population around Ambavala is designated as the source population for physical specimens in support of the holotype.

Type locality

Forest near the rural village of Ambavala (S 16° 12.307', E 49° 35.371'), in a community protected forest at about 342 m a.s.l. approx. 20 km west of Mananara North, Province of Analanjirofo, Madagascar.

814 Paratypes

815 (a) BD1, adult female, captured in the community protected forest of Antsiradrano (near
816 Ambavala) on 04 September 2017. Tissue and hair samples as well as photographs and
817 morphometric measurements are stored at the Institute of Zoology, University of Veterinary
818 Medicine Hanover, Germany.
819 (b) B13, adult male, captured in the community protected forest near Ambavala on 11 September
820 2017. Tissue and hair samples as well as photographs and morphometric measurements are stored
821 at the Institute of Zoology of the University of Veterinary Medicine Hanover in Germany.
822 It is planned that one physical specimen will be obtained as a further paratype in the near future
823 and that this specimen will then be deposited in the Museum of the Zoology, Department of the
824 University of Antananarivo, Madagascar.
825

826 Description

827 *Microcebus jonahi* is a large-bodied, reddish-brown and small-eared mouse lemur (Fig. 7).
828 This species has short and dense fur. The head is rufous colored with a darker brownish area
829 around the eyes which can slightly vary among individuals. A distinct white stripe lies between
830 the eyes ending at the forehead (Fig. 7C). The ears are of the same rufous color as the head.
831 The cheeks are lighter brownish and less rufous than the head becoming even lighter and almost
832 white towards the throat. The ventrum is white with slightly yellowish nuances (Fig. 7D)
833 which can vary in appearance among individuals. The dorsum is rather uniformly brown than
834 reddish (Fig. 7E). A darker dorsal stripe can be either present or absent. The ventrum and
835 dorsum are separated by a significant change in coloration with only marginal transition. The
836 coloration of the limbs shows the same pattern with a brownish dorsal and a white to slightly
837 yellowish ventral side. The tail is densely furred and of the same coloration as the dorsum. Hands

838 and feet show only sparse but whitish-gray hair. The skin on the palmar and plantar surfaces of
839 hands and feet is brownish-pink. Males and females do not show any sexual dimorphism.

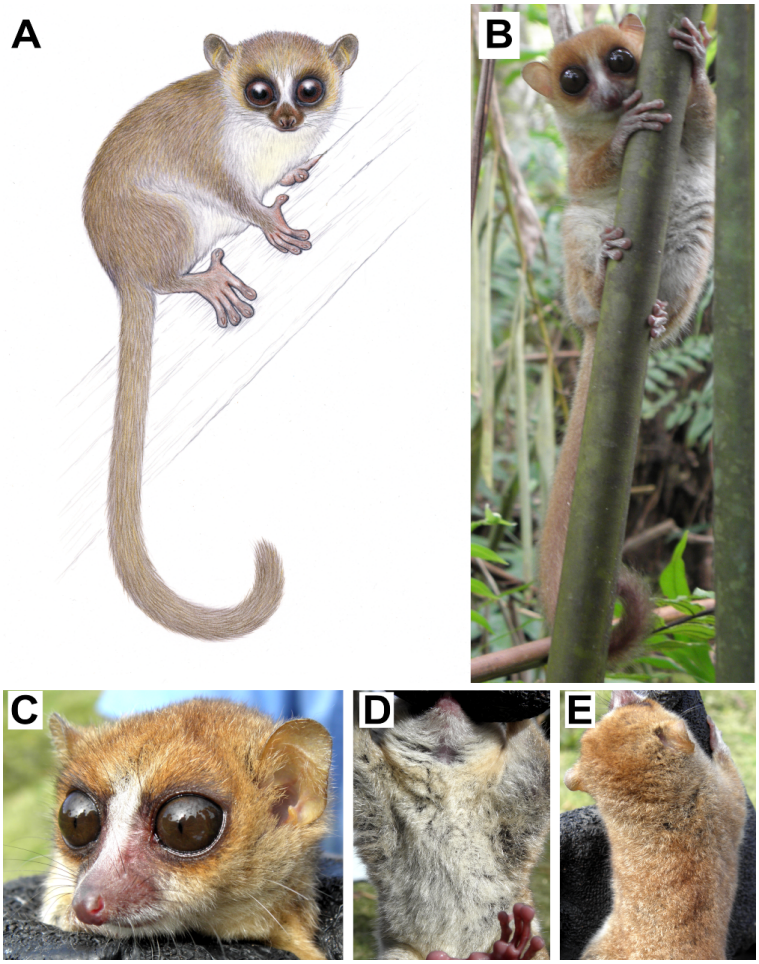

840

841 **Figure 7:** Outer morphology of *Microcebus jonahi*. **(A)** Drawing of an adult individual; **(B)**
842 Habitus of adult female (paratype individual BD1); **(C-E)** Close-ups of adult male (holotype
843 B34). Illustration copyright by Stephen D. Nash / IUCN SSC Primate Specialist Group; used with
844 permission. Photos by D. Schüßler.

845

846 Diagnosis

847 *M. jonahi* can be distinguished from other taxa in northeastern Madagascar by morphometric and
848 genetic differences. Compared to its closest relative, *M. macarthurii*, *M. jonahi* has a larger snout

849 length, ear and head width as well as a larger intra- and inter-orbital distance. In addition, *M.*
850 *jonahi* can be easily differentiated from *M. macarthurii* by its ventral coloration which is rather
851 whitish (*Fig. 7*), but distinctly yellowish-orange in *M. macarthurii* (Radespiel et al. 2008;
852 Radespiel and Raveloson unpubl. data).
853 Moreover, it can be easily distinguished from the sympatric, small-bodied *M. lehilahytsara* (at
854 Ambavala) by its higher weight, larger body size and tail length. Finally, *M. jonahi* can be
855 differentiated from its southern geographical neighbor, *M. simmonsi*, by its larger head width as
856 well as wider inter- and intra-orbital distances. *M. jonahi* could be unambiguously distinguished
857 from the other four taxa in this study across all analyses of nuclear RADseq data (see above).
858 However, it may not be reliably distinguished from *M. macarthurii* based solely on mtDNA
859 sequences, likely due to some introgression of mtDNA from *M. jonahi* into *M. macarthurii* (see
860 above) in the past.
861
862 Etymology
863 *M. jonahi* is named in honor of Malagasy primatologist Professor Jonah Ratsimbazafy. He has
864 dedicated his life's work to the conservation of Malagasy lemurs. With both national and
865 international outreach to the scientific community (e.g., GERP, IPS, LemurPortal), to the public
866 of Madagascar (e.g., by initiating the World Lemur Festival), and to the political leaders of
867 Madagascar, he serves as an inspirational role model for young Malagasy students and scientists.
868 He provides hope for the future of Madagascar and for its iconic lemurs during very challenging
869 times.
870
871 Vernacular name
872 English name: Jonah's mouse lemur, French name: Microcèbe de Jonah, German

873 name: Jonah's Mausmaki.

874 **Acknowledgements**

875 This study was conducted under the research permit No. 197/17/MEEF/SG/DGF/DSAP/SCB.Re
876 (DS), 072/15/MEEMF/SG/DGF/DCB.SAP/SCB (MBB), 137/13/MEF/SG/DGF/DCB.SAP/SCB
877 (DWR), 175/14/MEF/SG/DGF/DCB.SAP/SCB (AM), kindly issued by the directeur du système
878 des aires protégées, Antananarivo and the regional authorities (Direction Régional de
879 l'Environnement, de l'Ecologie et de Forêts). We are endebted to J.H. Ratsimbazafy, N.V.
880 Andriaholinirina, C. Misandeau, B. Le Pors and S. Rasoloharijaona, for their help with
881 administrative tasks and to G. Besnard for facilitating this study. We thank our field assistants (I.
882 Sitrakarivo, C. Hanitriniaina and T. Ralantoharijaona) and the ADAFAM (Association Des Amis
883 de la Forêt d'Ambodiriana-Manompana) for their valuable help during sample collection. We
884 warmly thank the many local guides and cooks for sharing their incomparable expertise and help
885 in the field, *misaotra anareo jiaby*.
886 Funding was granted by the Bauer Foundation and the Zempelin Foundation of the "Deutsches
887 Stiftungszentrum" under grant no. T237/22985/2012/kg and T0214/32083/2018/sm to DS, Duke
888 Tropical Conservation Initiative Grant to ADY, and Duke Lemur Center/SAVA Conservation
889 research funds to MBB, the School of Animal Biology at The University of Western Australia to
890 AM, the Fundação para a Ciência e a Tecnologia, Portugal (PTDC/BIA-BEC/100176/2008,
891 PTDC/BIA-BIC/4476/2012, and SFRH/BD/64875/2009), the Groupement de Recherche
892 International (GDRI) Biodiversité et développement durable – Madagascar, the Laboratoire
893 d'Excellence (LABEX) TULIP (ANR-10-LABX-41) and CEBA (ANR-10-LABX-25-01, the
894 Instituto Gulbenkian de Ciência, Portugal to LC and JS, the ERA-NET BiodivERsA project:
895 INFRAGECO (Inference, Fragmentation, Genomics, and Conservation, ANR-16-EBI3-0014 &
896 FCT-Biodiversa/0003/2015) the LIA BEEG-B (Laboratoire International Associé –
897 Bioinformatics, Ecology, Evolution, Genomics and Behaviour, CNRS) to LC and JS. Further

898 financial support came from the Institute of Zoology, University of Veterinary Medicine
899 Hannover and UR acknowledges the long-term support of the late Elke Zimmermann for her
900 research activities on Madagascar. The genomic data were generated with funds from NSF DEB-
901 1354610 to ADY and DWW and from the EDB Lab to JS. ADY also gratefully acknowledges
902 support from the John Simon Guggenheim Memorial Foundation and the Alexander von
903 Humboldt Foundation. EELJ would like to acknowledge support from the Ahmanson Foundation
904 for the data generation. This work was performed in collaboration with the GeT core facility,
905 Toulouse, France (http://get.genotoul.fr), and was supported by France Génomique National
906 infrastructure, funded as part of "Investissement d'avenir" program managed by Agence
907 Nationale pour la Recherche (contract ANR-10-INBS-09). JS, UR & LC also gratefully
908 acknowledge support from the Get-Plage sequencing and Genotoul bioinformatics
909 (BioinfoGenotoul) platforms Toulouse Midi-Pyrenees.

References

Alexander, D.H., Novembre, J., and Lange, K. 2009. Fast model-based estimation of ancestry in unrelated individuals. *Genome Res.* **19**: 1655–1664.

Ali, O. A., O'Rourke, S. M., Amish, S. J., Meek, M. H., Luikart, G., Jeffres, C., and Miller, M. R. 2016. RAD capture (rapture): Flexible and efficient sequence-based genotyping. *Genetics* **202**: 389–400.

Angelis, K., & Dos Reis, M. 2015. The impact of ancestral population size and incomplete lineage sorting on Bayesian estimation of species divergence times. *Current Zoology* **61**: 874-885.

Barley, A. J., Brown, J. M., and Thomson, R. C. 2017. Impact of model violations on the inference of species boundaries under the multispecies coalescent. *Syst. Biol.* **67**: 269–284.

Beaumont, M. A. 2004. Recent developments in genetic data analysis: What can they tell us about human demographic history? *Heredity* **92**: 365–379.

Boetzer, M., Henkel, C. V., Jansen, H. J., Butler, D., and Pirovano, W. 2011. Scaffolding pre-assembled contigs using sspace. *Bioinformatics* **27**: 578–579.

Brown, J. L. and Yoder, A. D. 2015. Shifting ranges and conservation challenges for lemurs in the face of climate change. *Ecol. Evol.* **5**: 1131–1142.

Bryant, D., Bouckaert, R., Felsenstein, J., Rosenberg, N. A., and RoyChoudhury, A. 2012. Inferring species trees directly from biallelic genetic markers: bypassing gene trees in a full coalescent analysis. *Mol. Biol. Evol.* **29**: 1917–1932.

Burney, D., James, H., Grady, F., Rafamantanantsoa, J. G., Wright, H., and Cowart, J. 1997. Environmental change, extinction and human activity: evidence from caves in NW Madagascar. *J. Biogeogr.* **24**: 755–767.

933 Campbell, C. R., Poelstra, J. W., and Yoder, A. D. 2018. What is speciation genomics? The roles
934 of ecology, gene flow, and genomic architecture in the formation of species. *Biol. J. Linn.*
935 *Soc.* **124**: 561–583.
936 Campbell, C. R., Tiley, G. P., Poelstra, J. W., Hunnicutt, K. E., Larsen, P. E., dos Reis, M., and
937 Yoder, A. D. 2019. Pedigree-based measurement of the de novo mutation rate in the gray
938 mouse lemur reveals a high mutation rate, few mutations in CpG sites, and a weak sex bias.
939 BiorXiv, posted August 5, 2019. doi: https://doi.org/10.1101/724880.
940 Chambers, E. A. and Hillis, D. M. 2019. The multispecies coalescent over-splits species in the
941 case of geographically widespread taxa. *Syst. Biol.* **68**: doi: org/10.1093/sysbio/syz042.
942 Chifman, J. and Kubatko, L. 2014. Quartet inference from SNP data under the coalescent model.
943 *Bioinformatics* **30**: 3317–3324.
944 Chikhi, L., Sousa, V., Luisi, P., Goossens, B., and Beaumont, M.A. 2010. The confounding
945 effects of population structure, genetic diversity and the sampling scheme on the detection
946 and quantification of population size changes. *Genetics* **186**: 983-995.
947 Chikhi, L., Rodríguez, W., Grusea, S., Santos, P., Boitard, S., Mazet, O. 2018. The IICR (inverse
948 instantaneous coalescence rate) as a summary of genomic diversity: insights into
949 demographic inference and model choice. *Heredity* **120**: 13-24.
950 Colombo, M., Damerau, M., Hanel, R., Salzburger, W., and Matschiner, M. 2015. Diversity and
951 disparity through time in the adaptive radiation of Antarctic notothenioid fishes. *J. Evol.*
952 *Biol.* **28**: 376–394.
953 Coyne, J. and Orr, H. 2004. *Speciation*. Sinauer Associates, Sunderland.
954 Czekanski-Moir, J. E. and Rundell, R. J. 2019. The ecology of nonecological speciation and
955 nonadaptive radiations. *Trends Ecol. Evol.* **34**: 400–415.

956 Dalquen, D. A., Zhu, T., and Yang, Z. 2017. Maximum likelihood implementation of an
957 isolation-with-migration model for three species. *Syst. Biol.***66**: 379-398.
958 Dávalos, L. M. and Russell, A. L. 2014. Sex-biased dispersal produces high error rates in
959 mitochondrial distance-based and tree-based species delimitation. *J. Mammal.***95**: 781–791.
960 De Queiroz, K. 2007. Species concepts and species delimitation. *Syst. Biol.***56**: 879–886.
961 DePristo, M. A., Banks, E., Poplin, R., Garimella, K. V., Maguire, J. R., Hartl, C., Philippakis,
962 A. A., Del Angel, G., Rivas, M. A., Hanna, M., McKenna, A., Fennell, T. J., Kernytsky
963 A. M., Sivachenko, A. Y., Cibulskis, K., Gabriel, S. B., Altshuler, D., Daly, M. J. 2011. A
964 framework for variation discovery and genotyping using next-generation DNA sequencing
965 data. *Nat. Genet.* **43**: 491–498.
966 Displayr. 2018. flipMultivariates R package. URL https://github.com/Displayr/flipMultivariates
967 Dos Reis, M., Gunnell, G. F., Barba-Montoya, J., Wilkins, A., Yang, Z., and Yoder, A. D. 2018.
968 Using phylogenomic data to explore the effects of relaxed clocks and calibration strategies
969 on divergence time estimation: Primates as a test case. *Syst. Biol.***67**: 594–615.
970 Edwards, D. L. and Knowles, L. L. 2014. Species detection and individual assignment in species
971 delimitation: can integrative data increase efficacy? *Proc. Roy. Soc. B* **281**: 20132765.
972 Edwards, S. V., and Beerli, P. 2000. Gene divergence, population divergence, and the variance in
973 coalescent time in phylogeographic studies. *Evolution* **54**: 1839–1854.
974 Eriksson, A., and Manica, A. 2012. Effect of ancient population structure on the degree of
975 polymorphism shared between modern human populations and ancient hominins. *Proc. Natl.*
976 *Acad. Sci. USA* **109**: 13956-13960.
977 Estrada, A., Garber, P. A., Rylands, A. B., Roos, C., Fernandez-Duque, E., Di Fiore, A., Nekaris,
978 K. A. I., Nijman, V., Heymann, E. W., Lambert, J. E., Rovero, F., Barelli, C., Setchell, J. M.,
979 Gillespie, T. R., Mittermeier, R. A., Arregoitia, L. V., de Guinea, M., Gouveia, S.,

Dobrovolski, R., Shanee, S., Shanee, N., Boyle, S. A., Fuentes, A., MacKinnon, K. C., Amato, K. R., Meyer, A. L. S., Wich, S., Sussman, R. W., Pan, R., Kone, I., and Li, B. 2017. Impending extinction crisis of the worlds primates: Why primates matter. *Sci. Adv.* **3**: e1600946.

Fabre, A. C., Perry, J. M., Hartstone-Rose, A., Lowie, A., Boens, A., and Dumont, M. 2018. Do muscles constrain skull shape evolution in strepsirrhines? *Anat. Rec.* **301**: 291–310.

Feder, J. L., Egan, S. P., and Nosil, P. 2012. The genomics of speciation-with-gene-flow. *Trends Genet.* **28**: 342–350.

Flouri, T., Jiao, X., Rannala, B., and Yang, Z. 2018. Species tree inference with BPP using genomic sequences and the multispecies coalescent. *Mol. Biol. Evol.* **35**: 2585–2593.

Fox, J. and Weisberg, S. 2011. An R Companion to Applied Regression. Second Edition. Sage, Thousand Oaks CA. URL http://socserv.socsci.mcmaster.ca/jfox/Books/Companion

Fumagalli, M., Vieira, F. G., Korneliussen, T. S., Linderoth, T., Huerta-Sánchez, E., Albrechtsen, A., and Nielsen, R. 2013. Quantifying population genetic differentiation from next-generation sequencing data. *Genetics* **195**: 979-992.

Fumagalli, M., Vieira, F. G., Linderoth, T., and Nielsen, R. 2014. ngstools: methods for population genetics analyses from next-generation sequencing data. *Bioinformatics* **30**: 1486–1487.

Gasse, F. and Van Campo, E. 2001. Late quaternary environmental changes from a pollen and diatom record in the southern tropics (lake Tritrivakely, Madagascar). *Palaeogeogr. Palaeoclimatol. Palaeoecol.* **167**: 287–308.

Gavrilets, S. and Boake, C. R. 1998. On the evolution of premating isolation after a founder event. *Am. Nat.* **152**: 706–716.

1003 Gonen, S., Bishop, S. C., and Houston, R. D. 2015. Exploring the utility of cross-laboratory rad-
1004 sequencing datasets for phylogenetic analysis. *BMC Res. Notes* **8**: 299.
1005 Goodman, S. M. and Benstead, J. P. 2005. Updated estimates of biotic diversity and endemism
1006 for Madagascar. *Oryx* **39**: 73–77.
1007 Goodman, S. M. and Ganzhorn, J. U. 2004. Biogeography of lemurs in the humid forests of
1008 Madagascar: the role of elevational distribution and rivers. *J. Biogeogr.* 31:47–55.
1009 Goudet, J. 2005. Hierfstat, a package for R to compute and test hierarchical f-statistics. *Mol.*
1010 *Ecol. Notes* **5**: 184–186.
1011 Gronau, I., Hubisz, M. J., Gulko, B., Danko, C. G., and Siepel, A. 2011. Bayesian inference of
1012 ancient human demography from individual genome sequences. *Nat. Genet.* **43**: 1031–1034.
1013 Hackel, J., Vorontsova, M. S., Nanjarisoa, O. P., Hall, R. C., Razanatsoa, J., Malakasi, P., and
1014 Besnard, G. 2018. Grass diversification in Madagascar: In situ radiation of two large C_3
1015 shade clades and support for a Miocene to Pliocene origin of C_4 grassy biomes. *J. Biogeogr.*
1016 **45**: 750–761.
1017 Hafen, T., Neveu, H., Rumpler, Y., Wilden, I., and Zimmermann, E. 1998. Acoustically
1018 dimorphic advertisement calls separate morphologically and genetically homogenous
1019 populations of the grey mouse lemur (*Microcebus murinus*). *Folia Primatol.* **69**: 342–356.
1020 Harrison, R. G. and Larson, E. L. 2014. Hybridization, introgression, and the nature of species
1021 boundaries. *J. Hered.* **105**: 795–809.
1022 Heckman, K. L., Mariani, C. L., Rasoloarison, R., and Yoder, A. D. 2007. Multiple nuclear loci
1023 reveal patterns of incomplete lineage sorting and complex species history within western
1024 mouse lemurs (*Microcebus*). *Mol. Phylogenet. Evol.* **43**: 353–367.
1025 Heller, R., Chikhi, L., and Sigiesmund, H.R. 2013. The confounding effect of population
1026 structure on bayesian skyline plot inferences of demographic history. *PLoS ONE* **8**: e62992.

1027 Herrera, J. P. and Dávalos, L. M. 2016. Phylogeny and divergence times of lemurs inferred with
1028 recent and ancient fossils in the tree. *Syst. Biol.***65**: 772–791.
1029 Hey, J. and Nielsen, R. 2007. Integration within the Felsenstein equation for improved Markov
1030 chain Monte Carlo methods in population genetics. *Proc. Natl. Acad. Sci. USA* **104**: 2785–
1031 2790.
1032 Hey, J. and Pinho, C. 2012. Population genetics and objectivity in species diagnosis. *Evolution*
1033 **66**: 1413–1429.
1034 Hotaling, S., Foley, M. E., Lawrence, N. M., Bocanegra, J., Blanco, M. B., Rasoloarison, R.,
1035 Kappeler, P. M., Barrett, M. A., Yoder, A. D., and Weisrock, D. W. 2016. Species discovery
1036 and validation in a cryptic radiation of endangered primates: coalescent-based species
1037 delimitation in Madagascar's mouse lemurs. *Mol. Ecol.* **25**: 2029–2045.
1038 Huang, J.-P., Leavitt, S. D., and Lumbsch, H. T. 2018. Testing the impact of effective population
1039 size on speciation rates – a negative correlation or lack thereof in lichenized fungi. *Sci. Rep.*
1040 **8**: 5729.
1041 Jackson, N. D., Carstens, B. C., Morales, A. E., and O'Meara, B. C. 2017. Species delimitation
1042 with gene flow. *Syst. Biol.***66**: 799–812.
1043 Jombart, T. 2008. adegenet: a R package for the multivariate analysis of genetic markers.
1044 *Bioinformatics* **24**: 1403–1405.
1045 Jombart, T. and Ahmed, I. 2011. adegenet 1.3-1: new tools for the analysis of genome-wide SNP
1046 data. *Bioinformatics* **27**: 3070–3071.
1047 Kappeler, P., Rasoloarison, R., Razafimanantsoa, L., Walter, L., and Roos, C. 2005. Morphology,
1048 behaviour and molecular evolution of giant mouse lemurs (*Mirza* spp.) Gray, 1870, with
1049 description of a new species. *Primate Rep.* **71**: 3–26.
1050 Kass, R. E. and Raftery, A. E. 1995. Bayes factors. *J. Am. Stat. Assoc.***90**: 773–795.

1051 Khatri, B. S. and Goldstein, R. A. 2015. Simple biophysical model predicts faster accumulation
1052 of hybrid incompatibilities in small populations under stabilizing selection. *Genetics* **201**:
1053 1525–1537.
1054 Khatri, B. S. and Goldstein, R. A. 2018. Biophysics and population size constrains speciation in
1055 an evolutionary model of developmental system drift. *BioRxiv.* doi: 10.1101/123265.
1056 Kiage, L. M. and Liu, K. B. 2006. Late Quaternary paleo-environmental changes in East Africa:
1057 A review of multiproxy evidence from palynology, lake sediments, and associated records.
1058 *Prog. Phys. Geogr.* **30**: 633–658.
1059 Kim, B. Y., Wei, X., Fitz-Gibbon, S., Lohmueller, K. E., Ortego, J., Gugger, P. F., and Sork,
1060 V. L. 2018. RADseq data reveal ancient, but not pervasive, introgression between
1061 Californian tree and scrub oak species (*Quercus* sect. *Quercus*: *Fagaceae*). *Mol. Ecol.* **27**:
1062 4556–4571.
1063 Knoop, S., Chikhi, L., and Salmona, J. 2018. Mouse lemur's use of degraded habitat. *Lemur*
1064 *News* **21**: 20–31.
1065 Korneliussen, T. S., Albrechtsen, A., and Nielsen, R. 2014. Angsd: analysis of next generation
1066 sequencing data. *BMC Bioinformatics* **15**: 356.
1067 Kottek, M., Grieser, J., Beck, C., Rudolf, B., and Rubel, F. 2006. World map of the Köppen-
1068 Geiger climate classification updated. *Meteorol. Z.***15**: 259–263.
1069 Langmead, B., Trapnell, C., Pop, M., and Salzberg, S. L. 2009. Ultrafast and memory-efficient
1070 alignment of short DNA sequences to the human genome. *Genome Biol.* **10**: R25.
1071 Leaché, A., Zhu, T., Rannala, B., and Yang, Z. 2019. The spectre of too many species. *Syst.*
1072 *Biol.***68**: 168–181.
1073 Leaché, A. D., Fujita, M. K., Minin, V. N., and Bouckaert, R. R. 2014. Species delimitation using
1074 genome-wide SNP data. *Syst. Biol.***63**: 534–542.

1075 Lecompte, E., Crouau-Roy, B., Aujard, F., Holota, H., and Murienne, J. 2015. Complete
1076 mitochondrial genome of the gray mouse lemur, *Microcebus murinus* (Primates,
1077 *Cheirogaleidae*). *Mitochondrial DNA A* **27**: 3514–3516.
1078 Louis, E. E., Coles, M. S., Andriantompohavana, R., Sommer, J. A., Engberg, S. E., Zaonarivelo,
1079 J. R., Mayor, M. I., and Brenneman, R. A. 2006. Revision of the mouse lemurs (*Microcebus*)
1080 of eastern Madagascar. *Int. J. Primatol.* **27**: 347–389.
1081 Louis, E. E., Engberg, S. E., McGuire, S. M., McCormick, M. J., Randriamampionona, R.,
1082 Ranaivoarisoa, J. F., Bailey, C.A., Mittermeier, R. A., and Lei, R. 2008. Revision of the
1083 mouse lemurs, *Microcebus* (Primates, Lemuriformes), of northern and northwestern
1084 Madagascar with descriptions of two new species at Montagne d'Ambre National Park and
1085 Antafondro Classified Forest. *Primate Conserv.* **23**: 19–38.
1086 Louis, E. E. and Lei, R. 2016. Mitogenomics of the family *Cheirogaleidae* and relationships to
1087 taxonomy and biogeography in Madagascar. In: S. M. Lehman, U. Radespiel, and E.
1088 Zimmermann (Editors), *The Dwarf and Mouse Lemurs of Madagascar: Biology, Behavior*
1089 *and Conservation Biogeography of the Cheirogaleidae*, Chap. 3, Cambridge University
1090 Press, pp. 54–93.
1091 Lozier, J. D. 2014. Revisiting comparisons of genetic diversity in stable and declining species:
1092 assessing genome-wide polymorphism in North American bumble bees using RAD
1093 sequencing. *Mol. Ecol.* **23**: 788–801.
1094 Luo, A., Ling, C., Ho, S. Y. W., and Zhu, C. D. 2018. Comparison of methods for molecular
1095 species delimitation across a range of speciation scenarios. *Syst. Biol.***67**: 830–846.
1096 Maddison, W. P. 1997. Gene trees in species trees. *Syst. Biol.***46**: 523–536.
1097 Mallet, J., Besansky, N., and Hahn, M. W. 2016. How reticulated are species? *BioEssays* **38**:
1098 140–149.

1099 Martien, K. K., Leslie, M. S., Taylor, B. L., Morin, P. A., Archer, F. I., Hancock-Hanser, B. L.,
1100 Brittany, L., Rosel, P. E., Vollmer, N. L. Viricel, A., and Cipriano, F. (2017). Analytical
1101 approaches to subspecies delimitation with genetic data. *Mar. Mam. Sci.* 33:27-55.
1102 Martin, R. 1972. A preliminary field-study of the lesser mouse lemur (*Microcebus murinus* JF
1103 Miller 1777). *Z. Tierpsychol.* **9**: 43–89.
1104 Matute, D. R. 2013. The role of founder effects on the evolution of reproductive isolation. *J.*
1105 *Evol. Biol.* **26**: 2299–2311.
1106 Mayr, E. 1959. Isolation as an evolutionary factor. *Proc. Am. Phil. Soc.* **103**: 221–230.
1107 Mazet, O., Rodriguez, W. V., Grusea, S., Boitard, S., and Chikhi, L. 2016. On the importance of
1108 being structured: instantaneous coalescence rates and human evolution – Lessons for
1109 inference of ancestral population size? *Heredity* **116**: 362–371.
1110 McCormack, J. E., Heled, J., Delaney, K. S., Peterson, A. T., and Knowles, L. L. 2011.
1111 Calibrating divergence times on species trees versus gene trees: implications for speciation
1112 history of *Aphelocoma jays*. *Evolution* **65**: 184–202.
1113 Meloro, C., Cáceres, N. C., Carotenuto, F., Sponchiado, J., Melo, G. L., Passaro, F., and Raia, P.
1114 2015. Chewing on the trees: Constraints and adaptation in the evolution of the primate
1115 mandible. *Evolution* **69**: 1690–1700.
1116 Miller, A., Mills, H., Ralantoharijaona, T., Volasoa, N. A., Misandeau, C., Chikhi, L., Bencini,
1117 R., and Salmona, J. 2018. Forest type influences population densities of nocturnal lemurs in
1118 Manompana, northeastern Madagascar. *Int. J. Primatol.* **39**: 646–669.
1119 Myers, N., Mittermeier, R. A., Mittermeier, C. G., Da Fonseca, G. A., and Kent, J. 2000.
1120 Biodiversity hotspots for conservation priorities. *Nature* **403**: 853–858.

1121 Nater, A., Mattle-Greminger, M. P., Nurcahyo, A., Nowak, M. G., De Manuel, M., Desai, T., …,
1122 and Lameira, A. R. 2017. Morphometric, behavioral, and genomic evidence for a new
1123 orangutan species. *Current Biology* **27:** 3487-3498.
1124 Nielsen, R., Korneliussen, T., Albrechtsen, A., Li, Y., and Wang, J. 2012. SNP calling, genotype
1125 calling, and sample allele frequency estimation from new-generation sequencing data. *PLoS*
1126 *One* **7**: e37558.
1127 O'Leary, S. J., Puritz, J. B., Willis, S. C., Hollenbeck, C. M., and Portnoy, D. S. 2018. These
1128 aren't the loci you're looking for: Principles of effective SNP filtering for molecular
1129 ecologists. *Mol. Ecol.* **27**: 3193–3206.
1130 Olivieri, G., Zimmermann, E., Randrianambinina, B., Rasoloharijaona, S., Rakotondravony, D.,
1131 Guschanski, K., and Radespiel, U. 2007. The ever-increasing diversity in mouse lemurs:
1132 three new species in north and northwestern Madagascar. *Mol. Phylogenet. Evol.***43**: 309–
1133 327.
1134 Palkopoulou, E., Lipson, M., Mallick, S., Nielsen, S., Rohland, N., Baleka, S., Karpinski, E.,
1135 Ivancevic, A. M., To, T. H., Kortschak, R. D., Raison, J. M., Qu, Z., Chin, T.-J., Alt, K. W.,
1136 Claesson, S., Dalén, L., MacPhee, R. D. E., Meller, H., Roca, A. L., Ryder, O. A., Heiman,
1137 D., Young, S., Breen, M., Williams, C., Aken, B. L., Ruffier, M., Karlsson, E., Johnson, J.,
1138 Di Palma, F., Alfoldi, J., Adelson, D. L., Mailund, T., Munch, K., Lindblad-Toh, K.
1139 Hofreiter, M., Poinar, H., and Reich, D. 2018. A comprehensive genomic history of extinct
1140 and living elephants. *Proc. Natl. Acad. Sci. USA* **115**: E2566–E2574.
1141 Pamilo, P., and Nei, M. 1988. Relationships between gene trees and species trees. *Mol. Biol.*
1142 *Evol.* **5**: 568–583.
1143 Pastorini, J., Thalmann, U., and Martin, R. D. 2003. A molecular approach to comparative
1144 phylogeography of extant Malagasy lemurs. *Proc. Natl. Acad. Sci. USA* **100**: 5879–5884.

1145 Patterson, N., Moorjani, P., Luo, Y., Mallick, S., Rohland, N., Zhan, Y., Genschoreck, T.,
1146 Webster, T., and Reich, D. 2012. Ancient admixture in human history. *Genetics* **192**: 1065–
1147 1093.
1148 Payseur, B. A. and Rieseberg, L. H. 2016. A genomic perspective on hybridization and
1149 speciation. *Mol. Ecol.* **25**: 2337–2360.
1150 Pedersen, C. E. T., Albrechtsen, A., Etter, P. D., Johnson, E. A., Orlando, L., Chikhi, L.,
1151 Siegismund, H. R., and Heller, R. 2018. A southern African origin and cryptic structure in
1152 the highly mobile plains zebra. *Nat. Ecol. Evol.* **2**: 491–498.
1153 Quéméré, E., Amelot, X., Pierson, J., Crouau-Roy, B., and Chikhi, L. 2012. Genetic data suggest
1154 a natural pre-human origin of open habitats in northern Madagascar and question the
1155 deforestation narrative in this region. *Proc. Natl. Acad. Sci. USA* **109**: 13028–13033.
1156 Radespiel, U. 2016. Can behavioral ecology help us to understand the divergent geographic range
1157 sizes of mouse lemurs? In: S. M. Lehman, U. Radespiel, and E. Zimmermann (Editors), *The*
1158 *Dwarf and Mouse Lemurs of Madagascar: Biology, Behavior and Conservation*
1159 *Biogeography of the Cheirogaleidae*, Chap. 26, Cambridge University Press, pp. 498-519.
1160 Radespiel, U., Lutermann, H., Schmelting, B., and Zimmermann, E. (in revision): An empirical
1161 estimate of the generation time of mouse lemurs. *Am. J. Primatol.*
1162 Radespiel, U., Olivieri, G., Rasolofoson, D. W., Rakotondratsimba, G., Rakotonirainy, O.,
1163 Rasoloharijaona, S., Randrianambinina, B., Ratsimbazafy, J. H., Ratelolahy, F.,
1164 Randriamboavonjy, T., Rasolofoharivelo, T., Craul, M., Rakotozafy, L., and Randrianarison,
1165 R. M. 2008. Exceptional diversity of mouse lemurs (*Microcebus* spp.) in the Makira region
1166 with the description of one new species. *Am. J. Primatol.* **70**: 1033–1046.
1167 Radespiel, U., Ratsimbazafy, J. H., Rasoloharijaona, S., Raveloson, H., Andriaholinirina, N.,
1168 Rakotondravony, R., Randrianarison, R. M., and Randrianambinina, B. 2012. First

1169 indications of a highland specialist among mouse lemurs (*Microcebus* spp.) and evidence for
1170 a new mouse lemur species from eastern Madagascar. *Primates* **53**: 157–170.
1171 Radespiel, U., Sarikaya, Z., Zimmermann, E., and Bruford M.W. (2001) Sociogenetic structure in
1172 a free-living nocturnal primate population: sex-specific differences in the grey mouse lemur
1173 (*Microcebus murinus*). *Behav. Ecol. Sociobio*. 50: 493-502.
1174 Rannala, B. and Yang, Z. 2003. Bayes estimation of species divergence times and ancestral
1175 population sizes using DNA sequences from multiple loci. *Genetics* **164**: 1645–1656.
1176 Rannala, B. and Yang, Z. 2013. Improved reversible jump algorithms for Bayesian species
1177 delimitation. *Genetics* **194**: 245–253.
1178 Rasoloarison, R. M., Goodman, S. M., and Ganzhorn, J. U. 2000. Taxonomic revision of mouse
1179 lemurs (*Microcebus*) in the western portions of Madagascar. *Int. J. Primatol.* **21**: 963–1019.
1180 Rasoloarison, R. M., Weisrock, D. W., Yoder, A. D., Rakotondravony, D., and Kappeler, P. M.
1181 2013. Two new species of mouse lemurs (*Cheirogaleidae*: *Microcebus*) from eastern
1182 Madagascar. *Int. J. Primatol.* **34**: 455–469.
1183 Rice, W. R. and Hostert, E. E. 1993. Laboratory experiments on speciation: What have we
1184 learned in 40 years? *Evolution* **47**: 1637–1653.
1185 Rodríguez, W., Mazet, O., Grusea, S., Arredondo, A., Corujo, J. M., Boitard. S., and Chikhi. L.
1186 2018. The IICR and the non-stationary structured coalescent: towards demographic inference
1187 with arbitrary changes in population structure. *Heredity* **121**: 663-678.
1188 Schiffels, S. and Durbin, R. 2014. Inferring human population size and separation history from
1189 multiple genome sequences. *Nat. Genet.* **46**: 919–925.
1190 Schüßler, D., Mantilla-Contreras, J., Stadtmann, R., Ratsimbazafy, J. H., and Radespiel, U.
1191 (under review) Determinants of deforestation and prediction of future forest loss in remote
1192 and rural north-eastern Madagascar. *Biodiv. Conserv*.

1193 Schüßler, D., Radespiel, U., Ratsimbazafy, J.H., and Mantilla-Contreras, J. 2018. Lemurs in a
1194 dying forest: Factors influencing lemur diversity and distribution in forest remnants of north-
1195 eastern Madagascar. *Biol. Conserv.* **228**: 17–26.
1196 Schwitzer, C., Mittermeier, R.A., Johnson, S.E., Donati, G., Irwin, M., Peacock, H.,
1197 Ratsimbazafy, J., Razafindramanana, J., Louis Jr., E. E., Chikhi, L., Colquhoun, I.C.,
1198 Tinsman, J., Dolch, R., LaFleur, M., Nash, S., Patel, E., Randrianambinina, B.,
1199 Rasolofoharivelo, T., Wright, P.C. 2014. Averting lemur extinctions amidst Madagascar's
1200 political crisis. *Science* **343**: 842-43.
1201 Skotte, L., Korneliussen, T. S., and Albrechtsen, A. 2013. Estimating individual admixture
1202 proportions from next generation sequencing data. *Genetics* **195**: 693–702.
1203 Solís-Lemus, C., Knowles, L. L., and Ané, C. (2015). Bayesian species delimitation combining
1204 multiple genes and traits in a unified framework. *Evol*. 69:492-507.
1205 Stamatakis, A. 2014. Raxml version 8: a tool for phylogenetic analysis and post-analysis of large
1206 phylogenies. *Bioinformatics* **30**: 1312–1313.
1207 Sukumaran, J. and Knowles, L. L. 2017. Multispecies coalescent delimits structure, not species.
1208 *Proc. Natl. Acad. Sci. USA* **114**: 1607–1612.
1209 Uyeda, J. C., Arnold, S. J., Hohenlohe, P. A., and Mead, L. S. 2009. Drift promotes speciation by
1210 sexual selection. *Evolution* **63**: 583–594.
1211 Venables, W. N. and Ripley, B. D. 2002. *Modern Applied Statistics with S.* Fourth Edition.
1212 Springer, New York. ISBN 0-387-95457-0. URL http://www.stats.ox.ac.uk/pub/MASS4
1213 Viguier, B. 2004. Functional adaptations in the craniofacial morphology of Malagasy primates:
1214 shape variations associated with gummivory in the family *Cheirogaleidae*. *Ann. Anat.* **186**:
1215 495–501.

1216 Vorontsova, M. S., Besnard, G., Forest, F., Malakasi, P., Moat, J., Clayton, W. D., Ficinski, P.,
1217 Savva, G. M., Nanjarisoa, O. P., Razanatsoa, J., Randriatsara, F. O., Kimeu, J. M., Luke,
1218 W. R. Q., Kayombo, C., and Linder, H. P. 2016. Madagascar's grasses and grasslands:
1219 Anthropogenic or natural? *Proc. Roy. Soc. B* **283**: 20152262.
1220 Waeber, P. O., Wilmé, L., Mercier, J. R., Camara, C., and Lowry II, P. P. 2016. How effective
1221 have thirty years of internationally driven conservation and development efforts been in
1222 Madagascar? *PLoS One* **11**: e0161115.
1223 Warmuth, V. M., and Ellegren, H. 2019. Genotype-free estimation of allele frequencies reduces
1224 bias and improves demographic inference from RADSeq data. *Mol. Ecol. Resour.* **19**: 586–
1225 596.
1226 Weisrock, D. W., Rasoloarison, R. M., Fiorentino, I., Ralison, J. M., Goodman, S. M., Kappeler,
1227 P. M., and Yoder, A. D. 2010. Delimiting species without nuclear monophyly in
1228 Madagascar's mouse lemurs. *PLoS One* **5**: e9883.
1229 Wen, D., Yu, Y., Zhu, J., and Nakhleh, L. 2018. Inferring phylogenetic networks using PhyloNet.
1230 *Syst. Biol.***67**: 735–740.
1231 Wilmé, L., Goodman, S. M., and Ganzhorn, J. U. 2006. Biogeographic evolution of
1232 Madagascar's microendemic biota. *Science* **312**: 1063–1065.
1233 Xie, W., Lewis, P. O., Fan, Y., Kuo, L., and Chen, M. H. 2011. Improving marginal likelihood
1234 estimation for Bayesian phylogenetic model selection. *Syst. Biol.***60**: 150–160.
1235 Yang, Z., and Rannala, B. 2010. Bayesian species delimitation using multilocus sequence data.
1236 *Proc. Natl. Acad. Sci. USA* 107:9264–9269.
1237 Yang, Z., and Yoder, A. D. 2003. Comparison of likelihood and Bayesian methods for estimating
1238 divergence times using multiple gene loci and calibration points, with application to a
1239 radiation of cute-looking mouse lemur species. *Syst. Biol.* **52**: 705–716.

1240 Yoder, A. D., Campbell, C. R., Blanco, M. B., dos Reis, M., Ganzhorn, J. U., Goodman, S. M.,
1241 Hunnicutt, K. E., Larsen, P. A., Kappeler, P. M., Rasoloarison, R. M., Ralison, J. M.,
1242 Swofford, D. L., and Weisrock, D. W. 2016. Geogenetic patterns in mouse lemurs (genus
1243 *Microcebus*) reveal the ghosts of Madagascar's forests past. *Proc. Natl. Acad. Sci. USA* **113**:
1244 8049–8056.
1245 Yoder, A. D., Rasoloarison, R. M., Goodman, S. M., Irwin, J. A., Atsalis, S., Ravosa, M. J., and
1246 Ganzhorn, J. U. 2000. Remarkable species diversity in Malagasy mouse lemurs (*Primates*,
1247 *Microcebus*). *Proc. Natl. Acad. Sci. USA* **97**: 11325–11330.
1248 Zhang, C., Ogilvie, H. A., Drummond, A. J., and Stadler, T. 2017. Bayesian inference of species
1249 networks from multilocus sequence data. *Mol. Biol. Evol.* **35**: 504–517.
1250 Zhang, C., Zhang, D.X., Zhu, T., and Yang, Z. 2011. Evaluation of a bayesian coalescent method
1251 of species delimitation. *Syst. Biol.* **60**: 747–761.
1252 Zimin, A. V., Marçais, G., Puiu, D., Roberts, M., Salzberg, S. L., and Yorke, J. A. 2013. The
1253 MaSuRCA genome assembler. *Bioinformatics* **29**: 2669–2677.
1254 Zimmermann, E., Cepok, S., Rakotoarison, N., Zietemann, V., and Radespiel, U. 1998.
1255 Sympatric mouse lemurs in north-west Madagascar: A new rufous mouse lemur species
1256 (*Microcebus ravelobensis*). *Folia Primatol.* **69**: 106–114.
1257 Zimmermann, E., and Radespiel, U. 2014. Species concepts, diversity, and evolution in primates:
1258 lessons to be learned from mouse lemurs. *Evol. Anthropol.* **23**: 11–14.